Technical Report

TR-09-07

Sediment dynamics in the coastal areas of Forsmark and Laxemar during an interglacial

Lars Brydsten, Umeå University

June 2009

Svensk Kärnbränslehantering AB
Swedish Nuclear Fuel
and Waste Management Co

Box 250, SE-101 24 Stockholm
Phone +46 8 459 84 00

Sediment dynamics in the coastal areas of Forsmark and Laxemar during an interglacial

Lars Brydsten, Umeå University

June 2009

Keywords: Sediment dynamics, Bathymetry, Resuspension, Waves, Biosphere, Ecosystem, Sr-Site, Radionuclide.

Abstract

Radionuclides dissolved in groundwater that reach the sea bottom from below may bind to fine-grained particles. When a nuclide binds to an immovable particle in the sea sediment, further transport may cease; however, if the nuclide binds to a moveable particle it may be repeatedly suspended, transported, and re-deposited. Whether the nuclide binds to a moveable or immoveable particle determines the type of biota it encounters. Therefore, it is of great value to understand how bottom types are spread in the sea close to a proposed repository and how the distribution of these bottoms have changed over time, in order to predict what may happen if a nuclide leaks from a repository.

In the coastal areas of Forsmark and Laxemar, the sediment dynamics have been modelled for the period between 9500 BC and 9500 AD. The model is based on a wave model (STWAVE) included in the program package from SMS (Surface Water Modelling System). A sediment resuspension module was developed and is presented in this report. The model inputs are weather data (wind direction and wind speed) and bathymetry. The bathymetry is in a regular grid structure. The wave model is separated into two steps. The first is an outer model with coarse resolution (1000 m) that represents the whole Baltic Sea. This outer model gives border conditions to an inner model with higher resolution (100 m) that represents the coastal areas close to Forsmark and Laxemar. The outputs from the wave model are wave height, wave period and water depth for each cell in the model domains. A new program module, written in VisualBasic, reads the results from the wave module and calculates the maximum wave generated water velocity close to the sea bottom, and the maximum resuspendable grain size at that water velocity based on a semi-empirical relationship /Komar and Miller 1975/.

The model is run with a time step of 500 years. Since the bathymetry is changing over time due to the positive shore displacement, a sub-model for the Baltic Sea evolution has been evaluated within the project. It is based on a digital elevation model (DEM) covering the Baltic Sea and its surroundings (negative values for the sea and positive values for the land) that have also been evaluated within the project. The DEM is based on elevation data from many different sources that is merged into a common coordinate system and a common height system. These irregularly spaced data have been used to interpolate a regular DEM. For each time step, this DEM has been corrected to those circumstances prevalent at that date using shore displacement equations for about 80 places around the Baltic Sea /Påsse 2001/. This correction accounts for the special conditions that existed during periods when the Baltic Sea was a lake.

The bathymetry of the high-resolution model domains at Forsmark and Laxemar are based on existing 20 m resolution DEMs. The change in bathymetry over time for these areas is calculated using the shore displacement equations for three sites close to each model site, a strategy that makes it possible to investigate the tilt of the landscape. This factor has some significance early and late in the modelled period.

It is impossible to run the model for all combinations of wind directions and wind speeds at each time step due to time reason, so only wind directions from long fetches and two critical wind speeds are simulated. The two critical wind speeds are expected to show changes in the extensions of three sea bottom types: 1) erosion bottoms where the resuspension frequency is so high that a particle is settled for maximum of one month, 2) accumulation bottoms where resuspension is not occurring, and 3) transport bottoms where a particle can be settled for one month to 500 years. The higher wind speed is chosen so that it possibly occurs at least at one occasion each 500 years with a wind direction approximately parallel with the longest fetch and with duration enough to make the fetch the only limiting factor for the wave generation. The lower wind speed is chosen so that it occurs at least once a month this with a wind direction parallel with the longest fetch.

The validation of the wave module has been performed with data from the wave buoy situated at Finngrundet in the Bothnian Sea and the validation turned out well with less than 5% errors. The combined model (wave module and resuspension module) have been calibrated against marine geological data from Forsmark and validated against marine geological data from Laxemar. The validation turned out with satisfactory results: about 92% of the model domain area was classified correctly.

The simulation result shows a large variation over time in the extensions of the three bottom types. Generally, accumulation exists partly on bottoms with large water depths and partly on shallow bottoms inside the belt of the skerries which are sheltered from wave power. Erosion exists on shallow bottoms exposed to waves and transport is evident at all places between these two extremes, i.e. bottoms at intermediate depths with moderate wave exposure. Any single cell within the model domain has a characteristic evolution over time, beginning with accumulation due to a large water depth early after the ice melted off, then a period with transport, after that erosion when the water depth decreased even more, and finally back to transport and accumulation during a short period before the sea bottom becomes land. The last two phases are due to a decrease in wave power caused both by a denser archipelago and a shorter fetch. In this general pattern, many variations can occur, anything from sites with accumulation throughout the whole period to sites that lack the two final phases and therefore erode before it becomes land. To predict how radionuclides emanating from a possible repository leakage migrate, it is of course important to know what type of sea bottom these nuclides enter and the evolution over time of these bottoms.

Sammanfattning

En del radionuklider som med grundvatten når havsbotten kan bindas till finkorniga partiklar. Bindningen kan vara stark, och i dessa fall styrs den fortsatta transporten i havet av hur bärarpartikeln rör sig. Somliga partiklar i havssedimentet ligger fast och om nukliden binder till den typen av partikel kommer också nukliden att ligga stilla. Partiklar på andra typer av havsbottnar kan utsättas för upprepade resuspensioner – transporter – redeponeringar för att slutligen hamna på en botten där den fastläggs. Hur radionukliden exponeras mot biota skiljer sig stort mellan dessa två rörelsemönster och även vilka halter som man kan förvänta sig i sedimentet för olika typer av bottnar. Det är därför viktigt att ha kunskap om hur olika bottnar fördelar sig i havet nära ett tänkt förvar, och även hur fördelningen av dessa bottnar förändras över tid, för att kunna förutse vad som kan hända vid ett eventuellt förvarsläckage.

Sedimentdynamiken i kustområdena kring Forsmark och Laxemar har modellerats för perioden 9500 BC–9500 AD. Kärnan i modellen är en vågmodell (STWAVE) som ingår i programpaketet från SMS (Surfacewater Modelling System) som kompletterats med en egentillverkad resuspensionsmodul. Ingångsdata till modellen utgörs av väderdata (vindriktning och vindstyrka) och av batymetri (i en reguljär gridstruktur). Vågmodellen är uppdelad i två steg; först en yttre, med grov upplösning (1000 m), som utgörs av hela Östersjön. Denna yttre modell ger randvillkor till en inre modell med finare upplösning (100 m), vilken utgörs av kustområdena i anslutning till de två platserna. Vågmodellen genererar våghöjd, vågperiod och vattendjup för varje cell i modelldomänen. En nyutvecklad modul, som är skriven i VisualBasic, läser in resultaten från vågmodellen och beräknar den maximala våggenererade vattenhastigheten nära botten samt den maximala kornstorlek som kan resuspendera vid den vattenhastigheten baserat på ett semi-empiriskt samband /Komar och Miller 1975/.

Modellen har körts med tidsteg om 500 år. Eftersom batymetrin p.g.a. strandförskjutningen förändras över tiden har en sub-modell för Östersjöns utveckling utvecklats inom projektet. Den utgår från en höjdmodell över Östersjön och dess angränsande landområden (negativa värden för vattendjup och positiva för land) som också utvecklats inom projektet och som bygger på data från ett stort antal källor som samlats i ett gemensamt koordinatsystem och tillika höjdsystem. Dessa irreguljära data har sedan interpolerats till en reguljär digital höjdmodell (Digital Elevation Model, DEM). För varje tidssteg har denna DEM korrigerats till de förhållanden som rådde vid just den tidpunkten med hjälp av ett 80-tal strandförskjutningsekvationer /Påsse 2001/. Här har också tagits hänsyn till de perioder som Östersjön varit en sjö med utvecklingen av tröskelhöjderna för de olika sjöstadierna.

Batymetrin i de högupplösta modelldomänerna nära Forsmark och Laxemar har utgått från befintliga höjdmodeller för områdena. Förändringen i batymetrin för dessa områden över tid har beräknats med strandförskjutningsekvationerna i vardera tre platser i närheten och därför också kunnat ta hänsyn till den tippning av landskapet som har viss betydelse tidigt och sent i undersökningsperioden.

Det har av tidsskäl varit omöjligt att simulera samtliga kombinationer av vindstyrka och vindriktning vid varje tidssteg varför endast vindriktningar över långa fetcher och två kritiska vindstyrkor har simulerats. De två kritiska vindstyrkorna förväntas särskilja förändringen i utbredning av tre olika bottentyper; *erosionsbottnar* där resuspensionsfrekvensen är så hög att en partikel ligger kvar maximalt under en månads tid, *accumulationsbottnar* där ingen resuspension sker samt *transportbottnar* där en partikel kan ligga kvar mellan en månad och 500 år. Den högre vindstyrkan valdes så att den sannolikt förekommer minst en gång per 500 år, med en vindriktning ungefär parallell med den längsta fetchen och med en duration som krävs för att enbart fetchen skall vara begränsande för våguppbyggnaden. Den lägre vindstyrkan valdes så att den förekom minst en gång per månad också den med en vindriktning parallellt med den längsta fetchen.

Hur vindklimatet och isförhållanden varierat under holocen är okänt, likaledes hur vindklimatet och isförhållandena kommer förändras i framtiden. Därför har nuvarande förhållanden fått gälla för hela undersökningsperioden. Utifrån data gällande den geostrofiska vinden för ett stort antal platser under en 15-års period och isförhållandena i Östersjön under samma period har de två avgränsande vindstyrkorna valts till 10 respektive 25 m s^{-1}. Båda vindstyrkorna är konservativt valda för att inte riskera att överskatta erosionsbottnarnas utbredning eller att underskatta accumulationsbottnarnas area.

Validering av vågmodulen har utförts mot vågdata från Finngrundet i Bottenhavet där SMHI har en mätstation. Valideringen utföll med mycket goda resultat. Den kombinerade modellen (vågmodulen och resuspensionsmodulen) har kalibrerats mot maringeologiska data från Forsmark och validerats mot maringeologiska data från Laxemar. Även denna validering utföll med utmärkta resultat, cirka 92 % av modelldomänen har klassificerats korrekt.

Resultaten från modelleringarna visar på en stor variation över tid i de tre bottentypernas utbredning. Generellt förekommer accumulationsbottnar dels på stora vattendjup och dels i vågskyddade lägen inomskärs. Erosionsbottnar förekommer i vågexponerade tämligen grunda lägen och transportbottnar i alla lägen mellan dessa två extremer, d.v.s. i mellanliggande områden med varken grunt eller djupt vatten och med måttlig vågexponering. En enskild plats i modellområdet får en karakteristisk utveckling över tid; inledningsvis förekommer accumulationsbotten eftersom vattendjupet är stort tidigt efter isavsmältningen. Efterhand som vattendjupet minskar övergår platsen till att vara en transportbotten. När vattendjupet minskar ytterligare följer en period med erosion, därefter bildas på nytt en transportbotten och när vågenergin avtar både p.g.a. den skärgård som uppstår vid en uppgrundning och en minskande fetch slutligen en accumulationsbotten på nytt. Variationer i detta generella mönster förekommer, allt från platser som har accumulationsbotten över hela perioden till platser som saknar den sista omvända utvecklingen och alltså har erosionsbotten när platsen övergår till land. För att förutse dynamiken av radionuklider som har ett ursprung från ett eventuellt läckande förvar, är det givetvis utomordentligt viktigt att veta om dessa når havsbotten på en plats med den förra eller senare typen av bottenutveckling.

Contents

1 Introduction

1.1 Background

If a leakage of radionuclides should occur from the deep repository, it may reach the biosphere at the sea bottom either directly through the bedrock at the sea bottom or indirectly by fluvial processes. Most of the radionuclides that reaches the sea bottom will be associated with clay particles or organic complexes. For some radionuclides the association is strong, so to understand how these radioactive compounds move, it is necessary to know the dynamics of these "carrier particles".

Most radionuclides are only bound to fine-grade particles or organic complexes so this study is only focused on the dynamics of cohesive particles (grain size < 0.02 mm). The dynamics of these particles are controlled by both wind-generated waves and baroclinic currents. In non-tidal areas, particles are normally resuspended from the sea bottom by the wave orbital water motion and transported by unidirectional currents. Less often particles are resuspended and transported solely by baroclinic currents. To model sediment dynamics it is necessary to model both wave-generated water motions and unidirectional currents simultaneously.

1.2 Objectives

The objectives for the modelling of sediment dynamics in coastal areas were concentrated to three issues:

- to model one inter-glacial period (~ 20,000 years) of the coastal areas of Forsmark and Laxemar in the Baltic Sea;
- to identify areas where fine-graded particles are permanently accumulated (accumulation bottoms) and areas where these particles cannot be accumulated (erosion bottoms) and determine how these areas change in extension over time; and
- to quantify the export and variation over time of fine-grained particles from the coastal areas to the open sea.

2 Methods and data

In an earlier study of the sediment dynamics in the Forsmark coastal area /Brydsten 1999/ used a wave model based on wave-ray techniques /May 1974, Brydsten 1985/. The main drawback of this study was that the wave-ray technique made it difficult to obtain model results for all parts of the study area; often small bays lacked model results. Recently, a number of different models have been developed that use finite difference or finite element techniques that do not have the failings of the wave-ray techniques and some models have also the opportunity to simultaneously run the wave model and the baroclinic current model. After a number of tests, a model package from "Surface Modelling Systems" (SMS-CMS) model package was chosen /McKee Smith et al. 2001/. The SMS-CMS software is a collection of models for use in coastal analysis. The models allow simulation of coastal currents, waves, and sediment transport.

The model STWAVE was chosen for wave modelling and M2D for modelling baroclinic currents. STWAVE simulates wave refraction and shoaling, wave breaking, diffraction, wave growth because of wind input, wave-wave interaction and white capping /McKee Smith et al. 2001/. M2D is a 2D, finite-difference hydrodynamic circulation model intended for analysis of coastal areas /Militello et al. 2004/.

The M2D model calculates the mean current velocity in the depth profile and transforms this to a velocity gradient in three depth layers. Later in the study, it was clear that this three-layer resolution was not sufficient to correctly model water movement close to the sediment surface. A beta 3D-version of the model was close to a final version, but was not available in time to be used in this study. The alternative SMS circulation model (ADCIRC) uses a sediment transport opportunity that was only intended to be used for frictional sediments and this model therefore lacks important parameters for cohesive sediments such as flocculation and size of non-spherical particles. After this shortcoming was uncovered, the analysis was carried out only based on waves and the third objective (export out from the coastal area) used with a different technique (discussed in Chapter 4).

The STWAVE model lacks a resuspension module so this module from the old wave model /Brydsten 1999/ was added to the STWAVE model.

2.1 Required input data to STWAVE

The STWAVE program requires the following input data:

(i) bathymetry,

(ii) wind speed,

(iii) wind direction, and

(iv) wind duration.

Since a complete interglacial period is modelled, the change in the Baltic Sea bathymetry over the same period must be calculated, including periods with fresh water (Baltic Ice Lake and Ancylus Lake) as well as the Ancylus transgression. A model for the Baltic Sea evolution does not exist, so this sub-model will be constructed within this study.

There is also a gap of knowledge concerning historical and future wind conditions in the Baltic region, so measured wind data for the last decades will be used for the whole period and the effects of possible long-time changes in wind climate during the interglacial on coastal sediment dynamics will be discussed in Chapter 4.

2.2 Wind data for the Baltic Sea

To calculate the probability of a certain wind speed from a certain direction a data set with geostrophic wind data was analyzed. The data set, which was provided from SMHI, gives geostrophic wind (speed and direction) for a large number of sites during the period 1990–2004. Out of approximately 900 stations, six were chosen for a more accurate analysis (see Figure 2-1). At each site (Forsmark and Laxemar), one station is chosen close to the model domain, one in the central part of the upwind area in the sea, and one in the remote upwind area.

A geostrophic wind is due to the Coriolis force blowing parallel to the isobars in the free atmosphere. The geostrophic wind must be converted to ground wind in order to be used as input for STWAVE. The standard method for this conversion is to multiply the wind speed with a factor 0.6 and turn the wind direction 15 degrees counter clockwise /Engqvist and Andrejev 1999/. The factor 0.6 is an average value for all ground types (open land, forest, water surface, etc). Therefore, the factor might be higher for solely water surfaces with a lower friction.

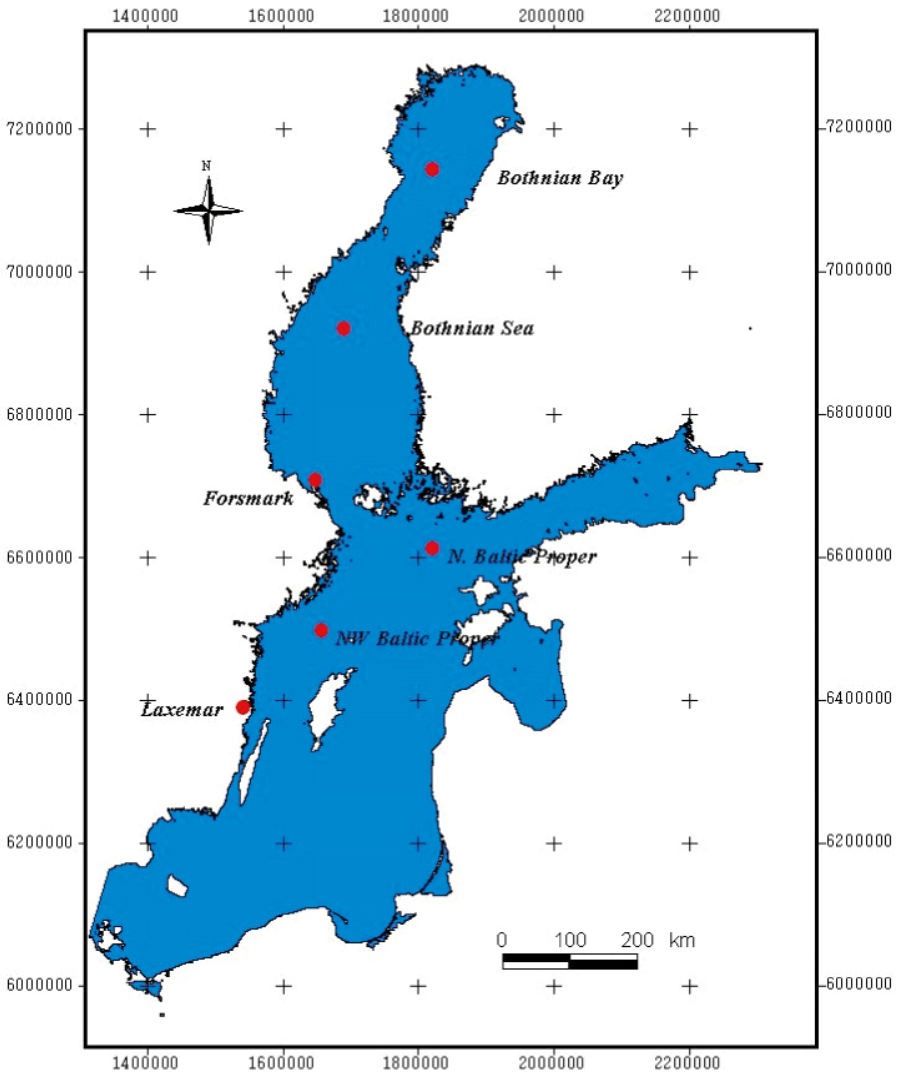

Figure 2-1. *Stations from the geostrophic data base chosen for analyzing probability of combinations of wind directions and wind speed. The coordinate system is RT90 2.5 gon W.*

One of the stations in the geostrophic wind data set coincided in space with the official weather station Örskär situated at the north cape of Gräsö, so it is here possible to compare ground wind data with geostrophic wind data. The two data sets have different time resolutions so a selection of data has been made from both data sets. The data set that is analyzed is from 2004 and has a time resolution of three hours: in total approximately 3000 records were analysed.

A statistical analysis of the relationship between ground wind speed and geostrophic wind speed shows that a factor of 0.75 is optimal for converting geostrophic wind speed to ground level at the Örskär site.

Figure 2-2 shows a comparison between measured wind speeds at ground surface (Örskär, 8 meters above ground) and the corrected modelled geostrophic wind speed (factor = 0.75) at approximately 8 km height.

The relationship is fairly strong with $r^2 = 0.70$ ($p < 0.01$) and the factor 0.75 will be used for the remaining analysis.

The winds that expect to give strong wave action in both sites are generated from wind directions from north to northeast. At Forsmark, waves from the east – south are sheltered by a dense archipelago. The big island Öland is sheltering the Laxemar site from all waves except from the north – northeast.

The frequency of wind speeds with wind directions from NW – ENE for six geostrophic wind stations are presented in Table 2-1. Maximum wind speeds various strongly between stations but are exceed 27 m s^{-1} at all stations. Wind speeds exceeding 10 m s^{-1} occur on average at all stations more than one per day, so from now on only wind durations for wind speeds higher than 10 m s^{-1} will be analyzed.

The relationship between wind speed (from NW – ENE) and wind duration for the geostrophic wind station close to Forsmark is shown in Table 2-2. High wind speeds only occur during short durations and at only one occasion the wind speed exceeded 20 m s^{-1} for more than one day.

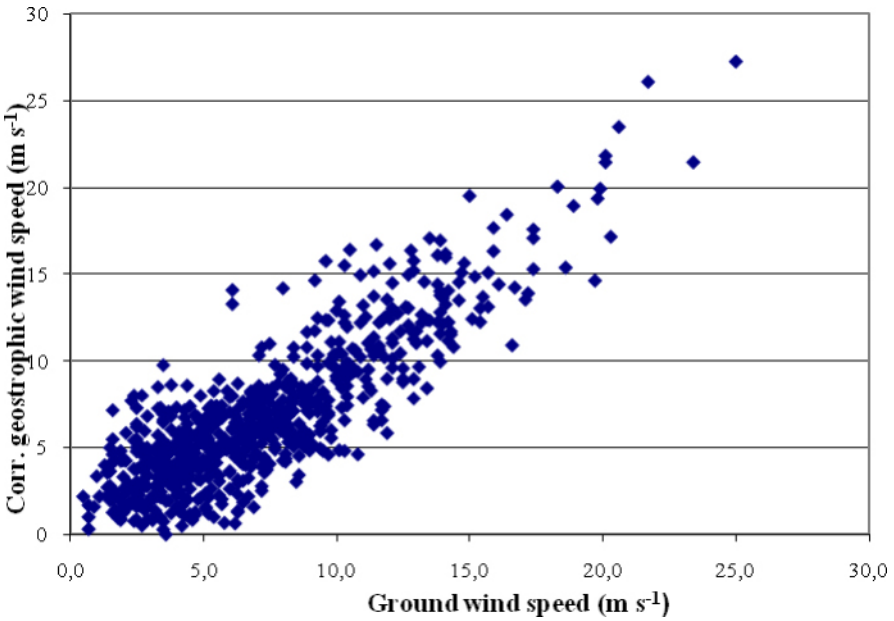

Figure 2-2. *The relationship between the corrected geostrophic wind speed (factor = 0.75) and measured wind speed at Örskär meteorological station.*

Table 2-1. Frequency of 3-hour events per year of wind speeds and wind directions from NW – ENE (340–70 º) for six geostrophic wind stations during the period 1990–2004 (see Figure 2-1). The geostrophic wind speeds are corrected using a factor of 0.75 and the wind directions are rotated 15 degrees counter clockwise.

Corr. Geostrophic Wind speed	Average fequency per year Laxemar	NW Baltic Proper	N Baltic Proper	Forsmark	Bothnian Sea	Bothnian Bay
> 1	431	513	673	505	312	487
> 2	429	511	671	503	311	486
> 3	425	510	669	500	307	484
> 4	420	507	666	495	304	480
> 5	415	504	661	490	301	476
> 6	409	499	655	484	297	472
> 7	402	493	648	476	292	465
> 8	394	486	637	464	286	456
> 9	380	469	615	446	274	438
> 10	349	435	573	408	248	403
> 11	282	359	486	329	192	329
> 12	227	293	408	262	146	265
> 13	179	235	337	205	108	211
> 14	139	184	275	158	78	165
> 15	106	143	223	120	55	127
> 16	79	109	178	91	36	96
> 17	57	83	142	68	24	72
> 18	41	61	111	50	16	52
> 19	28	44	87	38	10	37
> 20	20	31	67	28	6	26
> 21	14	22	52	21	3	18
> 22	9	15	39	16	2	12
> 23	5	10	29	12	1	7
> 24	3	7	21	9	1	5
> 25	2	5	16	6	< 1	3
> 26	1	3	12	5	< 1	2
> 27	< 1	2	9	4	< 1	1
> 28	< 1	1	6	3		1
> 29		< 1	5	2		< 1
> 30		< 1	4	2		< 1
> 31		< 1	3	1		< 1
> 32		< 1	3	1		
> 33			2	< 1		
> 34			2	< 1		
> 35			1	< 1		
> 36			1	< 1		
> 37			< 1	< 1		
> 38			< 1			
> 39			< 1			
> 40			< 1			

Table 2-2. Average number of yearly events at Forsmark with wind speeds (m s^{-1}) and wind durations (h) exceeding certain values. Only wind directions from 340–70º are analyzed.

	Duration								
Wind speed	> 6	> 9	> 12	> 15	> 18	> 21	> 24	> 27	> 30
> 10	384	307	245	197	160	130	106	86	69
> 11	289	226	177	140	111	88	69	54	42
> 12	217	166	127	97	74	57	44	34	26
> 13	153	113	84	62	46	34	25	18	13
> 14	109	79	56	41	29	21	15	11	8
> 15	76	54	38	26	18	12	8	5	3
> 16	52	35	23	15	10	6	4	2	1
> 17	37	24	15	9	5	3	1	< 1	
> 18	23	14	8	5	3	2	1	< 1	
> 19	15	8	5	3	2	1	< 1		
> 20	11	6	3	2	1	< 1	< 1		
> 21	8	4	2	1	1	< 1			
> 22	5	3	1	1	< 1	< 1			
> 23	3	2	1	< 1	< 1				
> 24	3	1	1	< 1	< 1				
> 25	2	1	< 1	< 1					
> 26	1	1	< 1	< 1					
> 27	1	1	< 1						
> 28	1	< 1	< 1						
> 29	< 1	< 1							
> 30	< 1								
> 31	< 1								
> 32	< 1								
> 33	< 1								
> 34	< 1								
> 35	< 1								
> 36	< 1								
> 37	< 1								

Tables with data similar to Table 2-2 for the other five stations are presented in Appendix.

2.3 Influence of sea ice on the generation of waves

Another limitation on the wave generation is the occurrence of sea ice. Solid ice at the sea shore decreases the fetch, giving lower waves than without any ice. In addition, solid or drift ice can absorb the energy of generated waves.

Generally, the Bothnian Bay is totally covered by ice each year, whereas in the Bothnian Sea and especially the Baltic Proper the covering rate varies significantly between different years. The freeze-up often starts in late October at the Finnish coast of the Bothnian Bay, continues growing westward in the Bothnian Bay and the eastern shore of the Bothnian Sea and the Archipelago Sea and the Gulf of Finland and along the Swedish coast of the Bothnian Sea and finally the central part of the Bothnian Sea. Some years also the northern part of the Baltic Proper is covered in ice (see Figure 2-3).

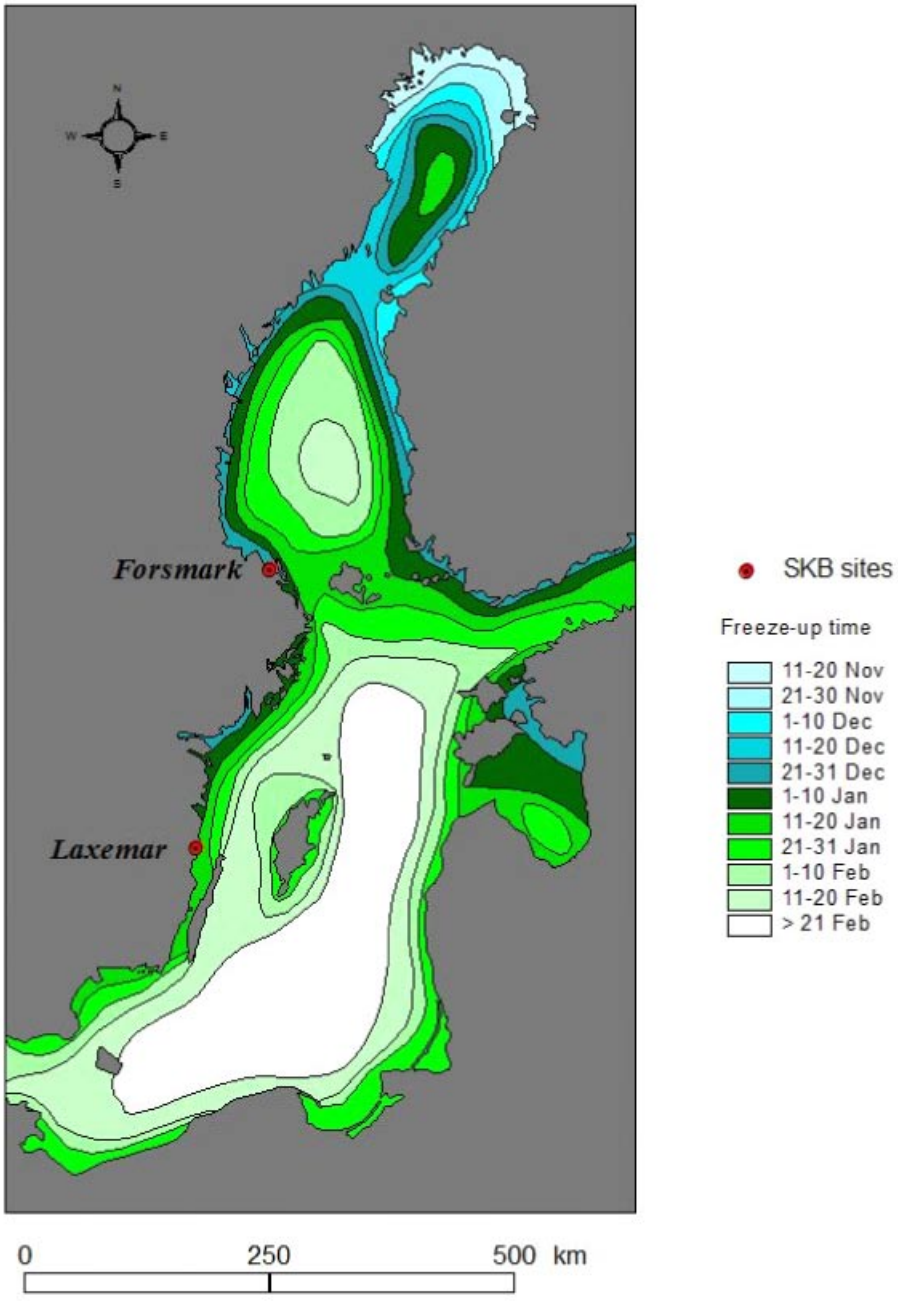

Figure 2-3. *Mean freeze-up time for the Baltic Sea during the period 1963–1979 (Redrawn from SNA PC-Atlasen GIS 2.0).*

The ice coverage duration has been calculated using data from Figure 2-3 and 2-4 (see Figure 2-5).

For a long time, the ice extensions have been registered remotely by satellite and this study uses data collected for the period 1990–2005. Each year from the date of first freeze-up, there are data for each third to fifth day until the date for a totally ice-free sea. The data are in a raster format with a cell size of 0.08 Nm in E-W and 0.04 Nm in N-S and covers the Baltic, the Danish Belt, Skagerrak, and Kattegat. The data is in a non-standard format, so a Visual Basic program has been constructed to convert data to a format readable in the ArcGis program.

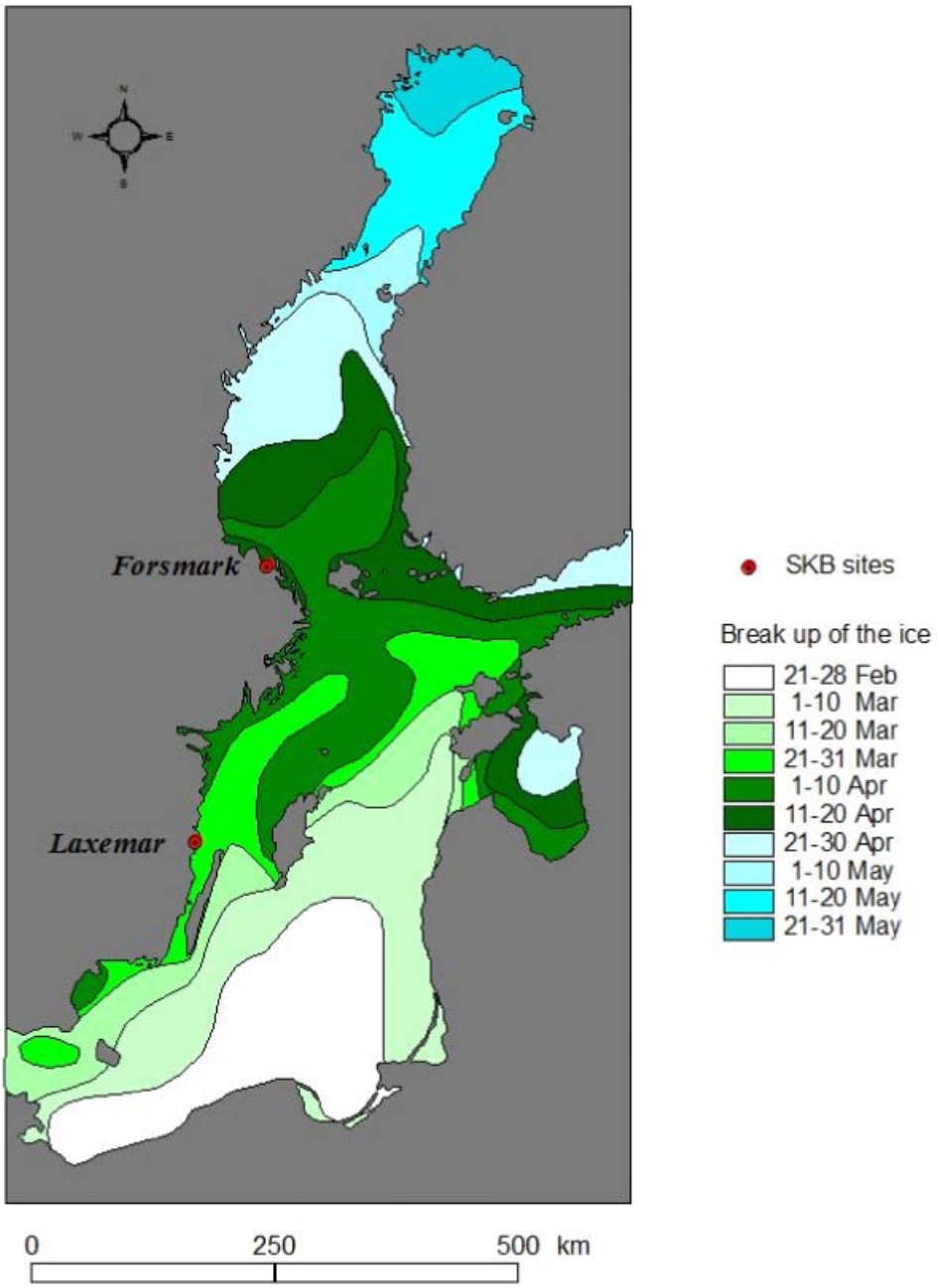

Figure 2-4. *Average dates for break-up of the ice in the Baltic Sea during the period 1963–1979 (Redrawn from SNA PC-Atlasen GIS 2.0).*

The first freeze-up in the Bothnian Sea normally occurs during the last two weeks in November or in December with the average of 7th of December during the period 1990–2005. The variation of the time for break-up is less and normally occurs in late April or early May with an average value of 1 May. The average time for ice coverage in the Bothnian Sea is 145 days.

The wave processes in the Laxemar model domain are affected by ice in the domain area and in the northern part of the Baltic Proper. The ice freeze-up date for the domain area is on average in late January and ice break-up date in late March, so the ice coverage duration is approximately two months. The average ice coverage duration in the wave generation area to Laxemar (the northern part of the Baltic Proper) is less than one month.

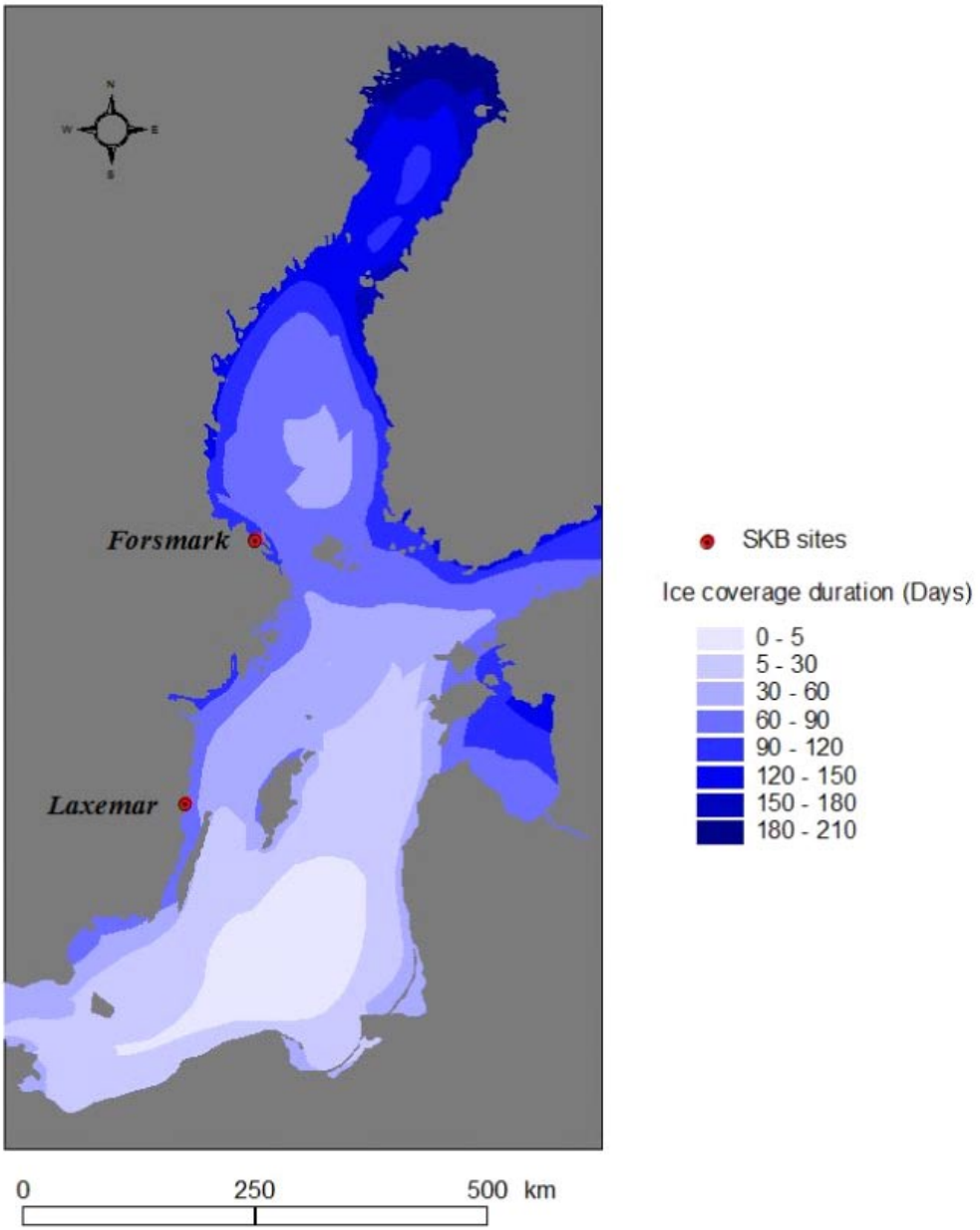

Figure 2-5. *Average ice coverage duration (days) for the Baltic Sea during the period 1963–1979.*

Since the ice coverage duration is more than twice as long at the Forsmark site than at the Laxemar site, the analysis of ice effect on wave processes will initially be done for the Forsmark site; if the affect is significant, the analysis will also be performed for the Laxemar site.

These figures are for first ice freeze-up and last break-up in the Bothnian Sea and cannot be used for calculations of probability for different combinations of wind duration and wind directions since large amounts of near shore ice outside the model domains (the regional area close to the sites) only are of minor importance for wave processes within the model domains while small amount of ice within the model domains can be of major importance for wave processes and therefore also for the sediment dynamics.

Therefore, the effect of each ice extension map on the wave processes within the model domains must be analyzed. In this respect following criteria have been used:

(i) if the fetch is decreased with less than 10% the wave processes is not effected; and

(ii) if some part of the model domains have solid or broken ice, the judgment is that no sediment dynamics occur.

One additional selection of wind data from Örskär (Wind speed > 10 m s^{-1} from 340–70 degrees) is made with these criteria. The further analysis of the probability of combinations of wind speed and wind directions will be done both for wind data corrected and uncorrected for ice. This is done to make it possible to estimate the effects of future climate change effect on the sediment dynamics.

The decrease in number of occasions of combinations of wind speed (U_{10}, wind speed at 10 meters height) and wind duration (t) for the data from Örskär during the period 2002–2005 after wind data has been corrected for ice (Table 2-3). The decrease is significant for low wind speeds and short durations, but small or non-existent for events with high wind speeds (compare with Table 2-2).

Ice coverage seems to reduce the wind speed so the extreme stormy events normally occur during ice-free periods, and therefore it is not necessary to pay attention to ice when determining the wind speed that will be used for modelling the extension of accumulation bottoms.

Since ice does not affect wave generation during stormy weather in Forsmark, it is assumed that Laxemar is not affected and the detailed analysis of ice conditions at this site is not accomplished.

2.4 Change in bathymetry in the Baltic Sea during the period 9500 BC–9000 AD

Bathymetry is a required input to the STWAVE program, partly with a high resolution within the model domains and partly with lower resolution for the entire Baltic Sea. The Baltic Sea bathymetry will be used in STWAVE for simulations of wave data that will be used as input data to the high-resolution STWAVE models at the sites.

Table 2-3. Decrease in number of occasions of combinations of wind speed (U_{10}, wind speed at 10 meters height) and wind duration (t) for the data from Örskär during the period 2002–2005 after wind data has been corrected for ice.

	U_{10} (m s^{-1})																
t (h)	>10	>11	>12	>13	>14	>15	>16	>17	>18	>19	>20	>21	>22	>23	>24	>25	>26
6–9	213	172	137	97	72	42	27	19	20	9	7	4	1	1	0	0	0
9–12	176	138	108	68	51	27	16	14	16	6	5	2	0	0			
12–15	147	111	87	50	35	20	12	11	13	4	3	0					
15–18	120	90	70	35	25	14	9	8	8	3	2						
18–21	98	75	57	26	16	10	7	6	4	2	1						
21–24	82	66	49	18	11	7	5	4	2	1	0						
24–27	70	57	40	11	8	4	3	2	1	0							
27–30	61	49	32	6	5	2	2	1	0								
30–33	53	41	25	2	2	1	1	0									
33–36	46	34	23	1	1	0	0										
36–39	38	26	12	0	0												
39–42	30	19	8														
42–45	24	13	5														
45–48	19	8	2														
48–51	14	3	0														
51–54	10	1															
54–57	6	0															
57–60	4																
60–63	3																
63–66	2																
66–69	1																
69–72	0																

The bathymetry of the Baltic Sea has been changed during the post-glacial period due to isostatic land uplift, eustatic sea level change, and erosion/accumulation of sediment bottoms. All three processes will continue, so the bathymetry will also be changed in the future. The change in bathymetry due to sedimentation processes is small compared to the eustatic and isostatic processes, so this factor will not be considered.

The shore level displacement (the sum of the eustatic and isostatic processes) is variable in different parts of the Baltic Sea and also of different rates over time. The Baltic Sea has also been a lake during two post-glacial periods (The Baltic Ice Lake and the Ancylus Lake), where the eustatic process had no affect on the bathymetry and only the isostatic processes determined the change.

The Baltic Sea bathymetry model (BSBM) was produced in three steps:

(1) A digital elevation model (DEM) for today's situation was produced. This DEM covers all land that at any time during the post-glacial period has been covered by Baltic Sea water.

(2) A model that describes the difference between today's elevation and the sea level elevation at any chosen time between 9500 BC and 9500 AD, with the same extension and resolution as the DEM, was developed. This is called a Shore level Displacement Model (SDM).

(3) The DEM for any chosen date was calculated as the difference between the present day DEM and the SDM for the chosen date.

2.4.1 A digital elevation model (DEM) for the Baltic Sea region

The data available for construction of a DEM covering the whole Baltic Sea are listed below:

(i) A DEM over land covering Sweden with a resolution of 50 meters in the Swedish national coordinate system RT90 2.5 gon W and the height system RH70.

(ii) Swedish coastal charts that also covers part of the Finnish coast of the Bothnian Bay and Bothnian Sea in the coordinate system WGS84 and various height systems that can be converted to RH70.

(iii) Swedish sea shorelines from the Swedish National Survey "Red map" in coordinate system RT90 2.5 gon W and height system RH70.

(iv) Baltic Sea shorelines from NGA (National Geospatial Intelligence Agency, www.nga.mil) in WGS84 and unknown height system but probably representing mean sea levels.

(v) A DEM covering the Baltic Sea from IOW (Baltic Sea Research Institute Warnemünde) /Seifert et al. 2001/ in geographical longitudes and latitudes in decimal degrees and unknown height system. The resolution is 2 minutes in longitude and 1 minute in latitude. http://www.io-warnemuende.de/research/en_iowtopo.html. The raw data to the DEM are from different sources but the part that covers the Gulf of Bothnia is stated to be in WGS84.

(vi) A DEM covering the Baltic Sea and surroundings from (National Geophysical Data Centre) with a resolution of 2 minutes in both longitude and latitude and in WGS84 coordinate system (http://www.ngdc.noaa.gov/mgg/gdas/gd_designagrid.html).

Data from all sources was converted to the RT90 2.5 gon W coordinate system with a central meridian of 13° 33' E, which is placed in the central part of the Baltic Sea. The choice of a plane coordinate system before a geographical (i.e. WGS84) is because it is simpler to calculate areas, distance, and angles in a plane system.

Many data sets are overlapping in space and therefore are the choices either to keep both or to delete the overlapping part of one of the datasets. The list above (i–vi) is sorted in estimated quality order, with the highest quality on top (i). The shoreline from NGA includes both the Swedish and Finnish coasts, whereas the shoreline from the "Red map" only covers the Swedish coast. Both data sets are in a vector format, but the data from the "Red map" has higher resolution (distance between vertexes), so data from the "Red map" is chosen for the Swedish coast and data from NGA for the rest of the area. Both datasets are converted in ArcGis from vector format to points by placing points at a distance of 100 meters along the lines.

The digital elevation models from IOW and NGDC include both land and water. The DEM for land areas in Sweden has both a higher resolution and a higher accuracy in the Z values, so data from IOW and NGDC were deleted for land areas in Sweden. For the remaining areas, the two data sets (IOW and NGDC) complement each other since they are to some degree displaced in both latitude and longitude directions and data from NGDC (with lower resolution); this approach fills in gaps in data from IOW. Both data sets are converted to points in shape-format. Because the two data sets are spatially joined together and data pairs are situated closer than 10 meters from each other, they are analyzed with respect to differences in Z-values. No large difference were found and there were no trends in the data sets (one of the data sets consequently larger than the other) so the data sets were merged into one single data set.

The merged data (IOW and NGDC) have a relatively coarse resolution, so data from Swedish sea charts were added this data set. The charts are in BBS-format, i.e. geo-referenced scanned paper charts. To get usable GIS-data, the depth values must be manually digitized. This is a very time consuming process so only areas critical for this study were digitized, namely the Northern Quark, Åland Sea, Archipelago Sea, the Danish Belts, and some shallow areas in the Bothnian Sea (e.g. the Finngrundet area). All point depths in these areas were digitized and the depth contours (3, 6, 10, 15, 20 and 50 meters) were digitized as points with an equidistance of approximately 100 meters. These data are estimated to have higher quality than data from IOW or NGDC, so data from IOW or NGDC closer than 100 meters from digitized data were deleted.

All data sets were merged into one single data set with attributes for Z (positive for land) and data source. The DEM was made by interpolation with Ordinary Kriging in ArcGis Geostatistical Analyst program (see Figure 2-6). The resolution was set to 500 meters.

2.4.2 Shore displacement in Fennoscandia during the period 9500 BC–9500 AD

An equation for shore displacement for Fennoscandia has been published by /Påsse 2001/. The equation is general but contains five parameters that are site specific. The equation is separated into three components: one eustatic (change in oceans levels over time) and one fast and one slow isostatic component (land uplift due to melting of the ice sheets). The eustatic component (E) is expressed as follows:

$$E = \frac{2}{\pi} * 56 * \left[Arc\tan\left(\frac{9500}{1350}\right) - Arc\tan\left(\frac{9500 - t}{1350}\right)\right] \quad \text{(Eq. 2-1)}$$

where t is the time BP in calendar years.

The slow isostatic component (U_S) is calculated as follows:

$$U_S = \frac{2}{\pi} * A_S * \left[Arc\tan\left(\frac{T_S}{B_S}\right) - Arc\tan\left(\frac{T_S - t}{B_S}\right)\right] \quad \text{(Eq. 2-2)}$$

where A_S is a down load factor (m), T_S is the time for maximal uplift rate, B_S is a inertia factor (y^{-1}) and t is the time in BP and calendar years

The fast isostatic component (U_F) is described as follows:

$$U_F = A_F * e^{-0.5*\left(\frac{t - T_F}{B_F}\right)^2} \quad \text{(Eq. 2-3)}$$

where A_F is the total uplift (m), B_F is an inertia factor (y^{-1}) and T_F is the time for the maximal uplift.

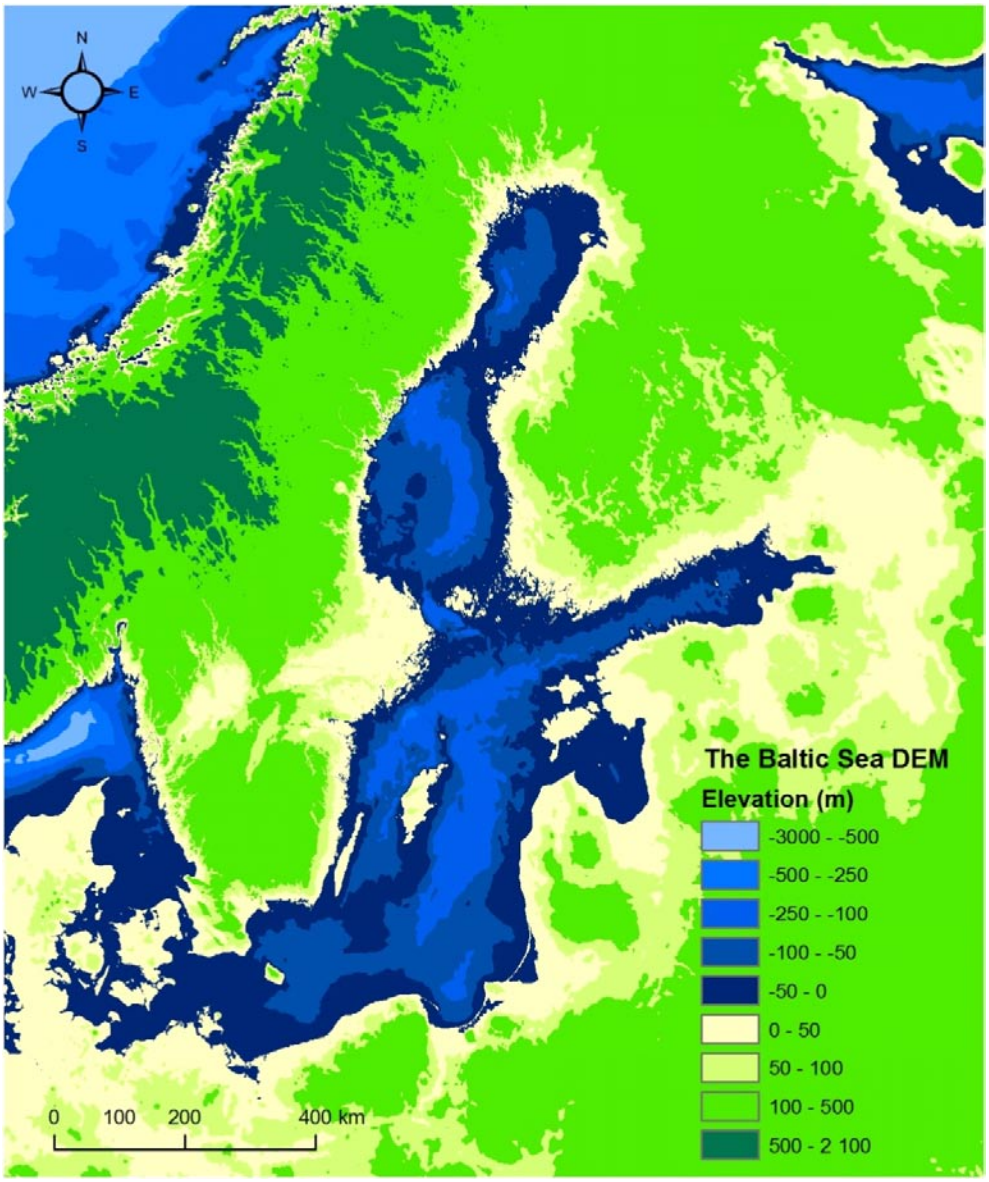

Figure 2-6. *A digital elevation model (DEM) for the Baltic Sea and its surroundings with a resolution of 500 meters.*

The total isostatic component (U) is calculated as follows:

$$U = U_S + U_F \quad \text{(Eq. 2-4)}$$

And finally, the shore displacement (S) is calculated as follows:

$$S = U - E \quad \text{(Eq. 2-5)}$$

The Baltic Sea has during two periods in Weichel been a lake *c.* 12,300–9600 BC as the Baltic Ice Lake and c. 8700–7300 BP as the Ancylus Lake. The equations 2.1–2.5 are only valid during the periods when the Baltic Sea was connected to the Atlantic, i.e. 9600–8700 BP as the Yoldia Sea and after 7300 BC as the Littorina Sea. During the lake periods the equations must be used with parameters associated with the lake thresholds.

Parameters for 72 sites distributed over Fennoscandia are presented in /Påsse 2001/ and parameters for Forsmark are given in /Brydsten 2006/ (see Figure 2-7).

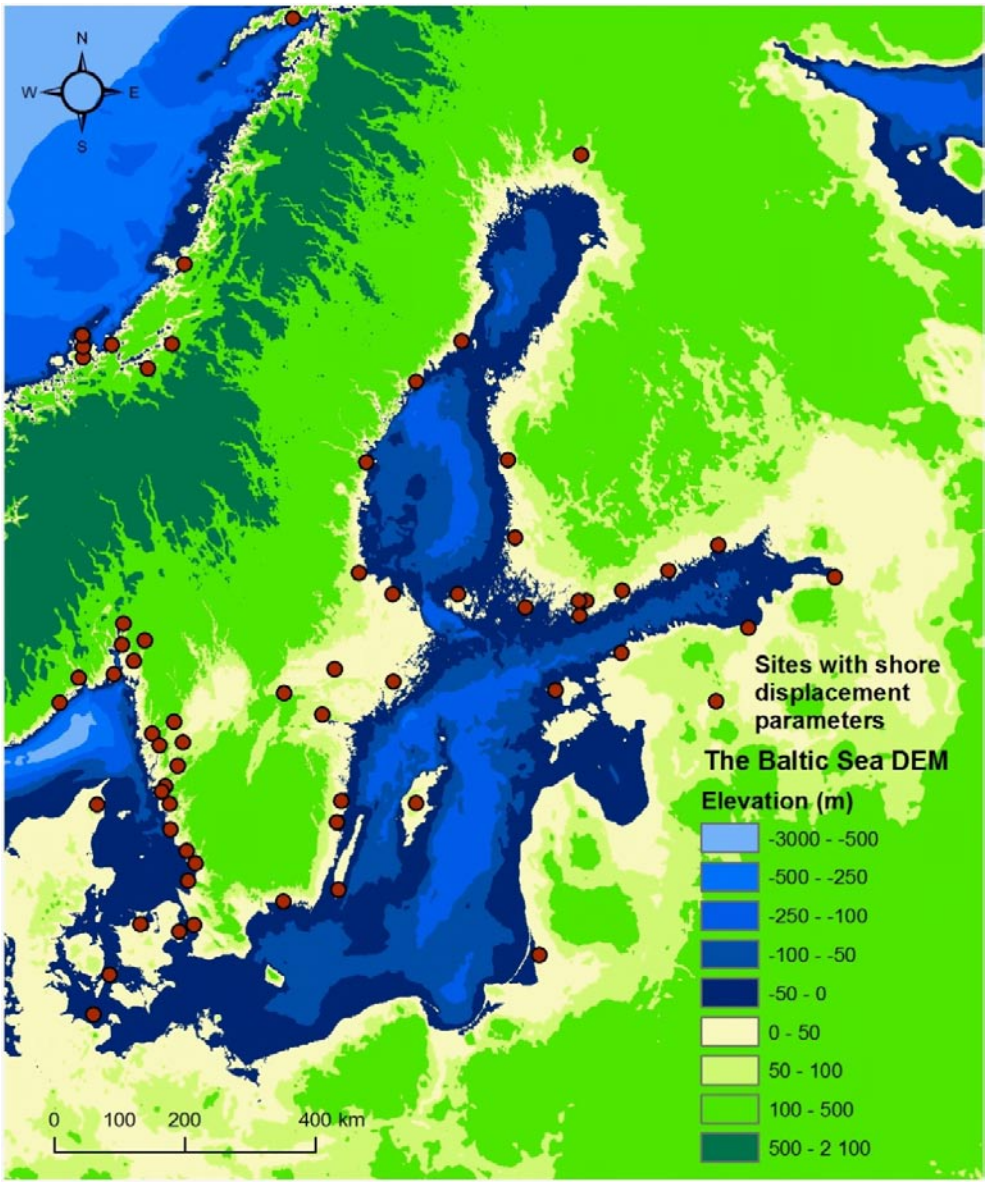

Figure 2-7. *Sites with shore displacement parameters /Påsse 2001, Brydsten 2006/.*

For each site, the shore level (S) has been calculated from 9500 BC to 9500 AD in 500 year steps using equation 2-1 to 2-5 and parameters from /Påsse 2001/ and /Brydsten 2006/. These S-values have been added to the attribute table of the site map (see Figure 2-7). For the time step 8500 BC the parameters from Degerfors and for the steps 8000 BC and 7500 BC the parameters for Dars Sill have also been used to calculate the Ancylus lake threshold level.

For each time step, a shore level raster map has been produced by interpolation using the U-values in the site map. This new raster map has exactly the same extension and resolution as the DEM. A DEM for a specific date is then produced by subtracting the DEM with the shore level map for that specific date. Figure 2-8 shows the DEM for the early post-glacial stage (9000 BC) and Figure 2-9 is a possible late stage of the inter-glacial period (9000 AD).

Figure 2-8. *A DEM for the Baltic region at the mid Ancylus stage (9000 BC). The red line represents the approximate extension of the ice sheet at c. 9000BC.*

2.4.3 The bathymetry in the model domains in Forsmark and Laxemar

The high-resolution SMS grids covering the coastal areas of Forsmark and Laxemar (100 meter resolution) are generated partly with a different method. The existing DEMs for the sites /Strömgren and Brydsten 2008a, b/ are in 20 meter resolution. The raw data for the 20 meter DEMs was used for interpolation of new 100 meter resolution grids. For each time-step, it is possible to use the shore displacement equations to recalculate the grid values for each site /Söderbäck (ed) 2008/, but the equations are only valid along a line perpendicular to the tilt of the shore displacement rate. Especially in the early interglacial period, the tilt was rather high and therefore must be taken into consideration.

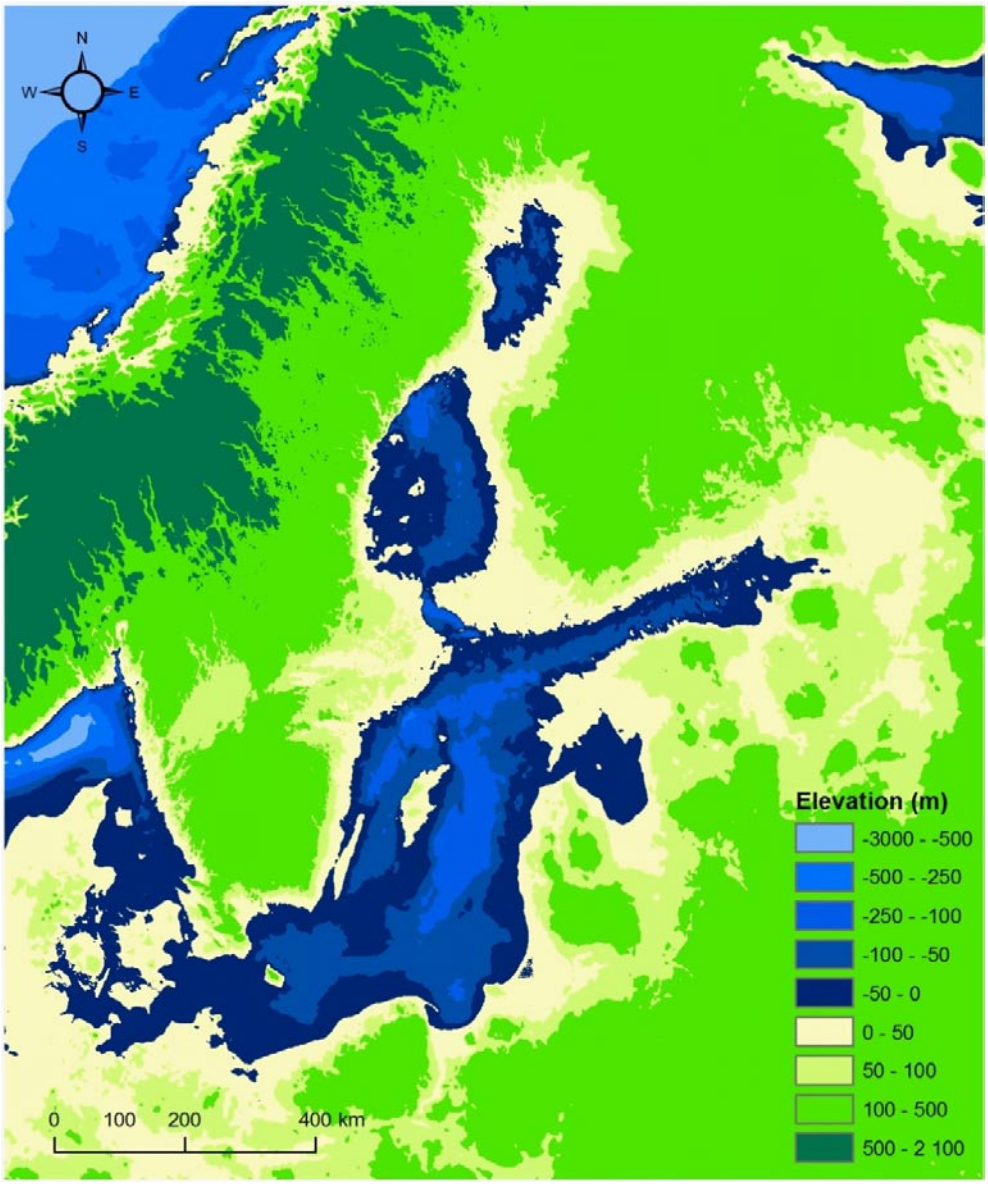

Figure 2-9. *A DEM for the Baltic region at 9000 AD.*

Figure 2-10 shows the closest sites to Forsmark with shore displacement equations /Påsse 2001/ and Figure 2-11 displays part of the shore displacement curves for these sites.

The tilt in shore displacement rate at the Forsmark site at different dates can be calculated using data from the sites Gästrikland, Stockholm area, and Åland. At each time step, the parameters for the sloping plane through the three sites can be calculated using the following equations:

$$A = ((Z_G - Z_S) \cdot (Y_S - Y_M) - (Z_S - Z_M) \cdot (Y_G - Y_S)) / ((X_G - X_S) \cdot (Y_S - Y_M) - (X_S - X_M) \cdot (Y_G - Y_S)) \quad \text{(Eq. 2-6)}$$

$$B = ((Z_G - Z_S) - A \cdot (X_G - X_S)) / (Y_G - Y_S) \quad \text{(Eq. 2-7)}$$

$$C = Z_G - (A \cdot X_G) - (B * Y_G) \quad \text{(Eq. 2-8)}$$

where A, B, and C are the parameters for the sloping plane, X is the E-W coordinate, Y is the N-S coordinate and the subscriptions G, S and M are the sites Gästrikland, Stockholm, and Åland (Mariehamn), respectively.

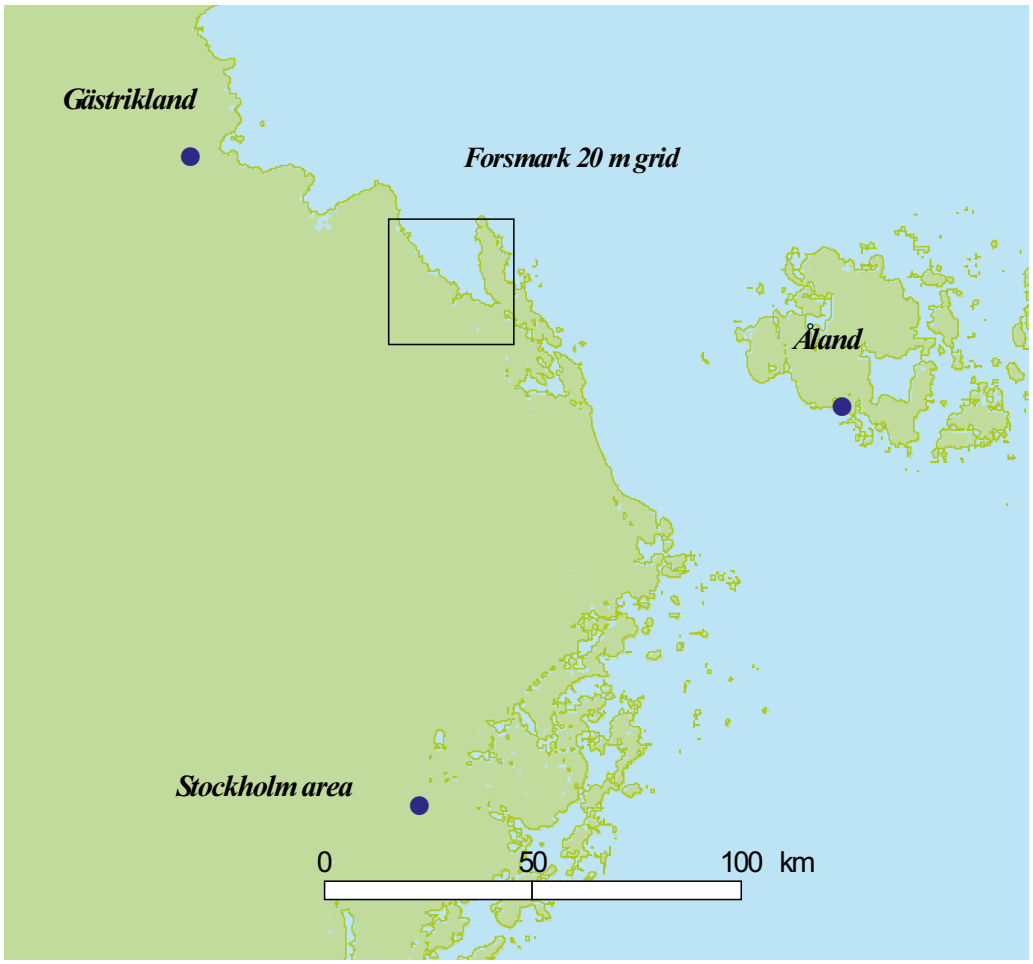

Figure 2-10. *Three sites close to Forsmark with known shore displacement equations.*

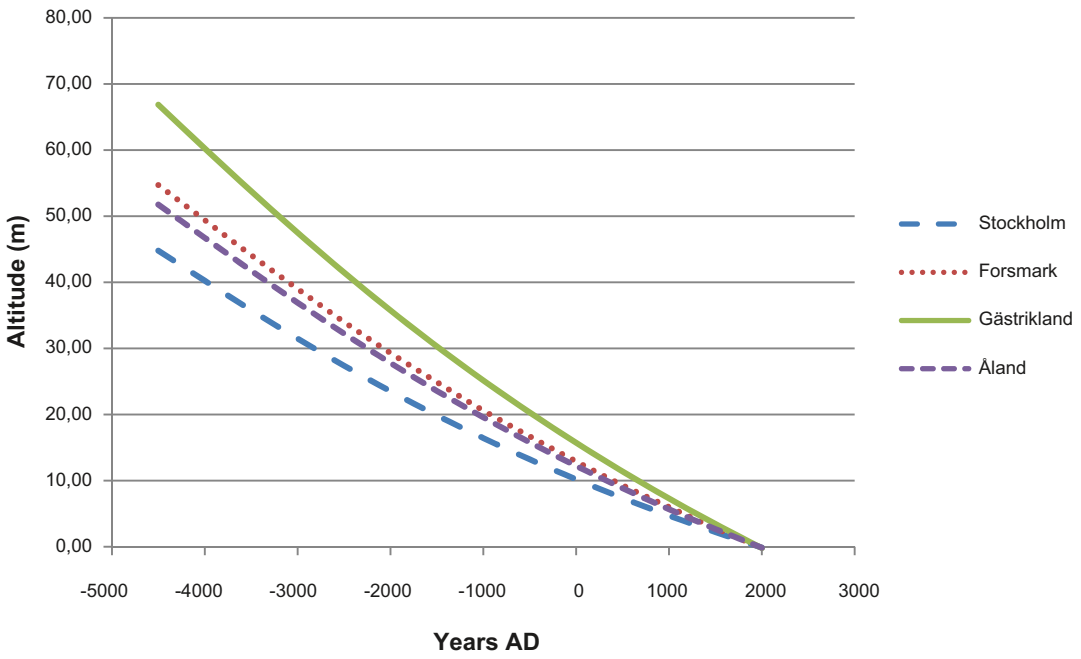

Figure 2-11. *Shore displacement curves for sites close to Forsmark.*

Using the parameters for the sloping plane the Z-value (altitude), dip and the dip azimuth can be calculated for each cell in the grid using the following equations:

$$\text{Z-value} = (A \cdot Y_{Cell}) + (B \cdot X_{Cell}) + C \quad \text{(Eq. 2-9)}$$

$$\text{Strike} = \text{Arctan}\,(A) \cdot (360/2\pi) \quad \text{(Eq. 2-10)}$$

$$\text{Dip Azimuth} = \text{Strike} - 90 \quad \text{(Eq. 2-11)}$$

$$\text{Dip} = \text{Arctan}\,((B/(\text{Cos}(\text{Strike}/(360/2\pi)))) \cdot (360/2\pi) \quad \text{(Eq. 2-12)}$$

where X_{Cell} and Y_{Cell} are the coordinates of the centre of the grid cell (RT90 2.5 gon W) and Strike, Dip Azimuth, and Dip are in degrees.

Both the dip and the dip azimuth vary over time so the recalculation of the Z-values in the grid must be based on unique sloping plane parameters for each time step. Therefore, a Visual Basic program was constructed that uses only date and the original DEM as input and generates a new DEM for the chosen date as the output.

The 20-meter shore displacement equation for the Forsmark site is based on data from /Hedenström and Risberg 2003/ and method from /Påsse 2001/. Using the VB-program for generating a shore displacement curve based on data from Gästrikland, Stockholm area, and Åland for two points in the NW and SE parts of the Forsmark grid gives curves that fit well with the data given by Hedenström and Risberg (see Figure 2-12). Due to the small differences between modelled and measured data, the model will be used for generating DEMs without any adjustments.

Figure 2-13 shows the shore displacement sites /Påsse 2001/ used for calculations of former and future DEMs at the Laxemar site. There are no measured shore displacement data within the Laxemar grid (radiocarbon dated isolation strata at levelled site) so that it is not possible to validate the Laxemar DEM generation model. Nevertheless, Figure 2-14 displays the modelled shore displacement curves for the NW and SE corners of the Laxemar grid. Also at this site, the maximum tilt occurs early in the interglacial.

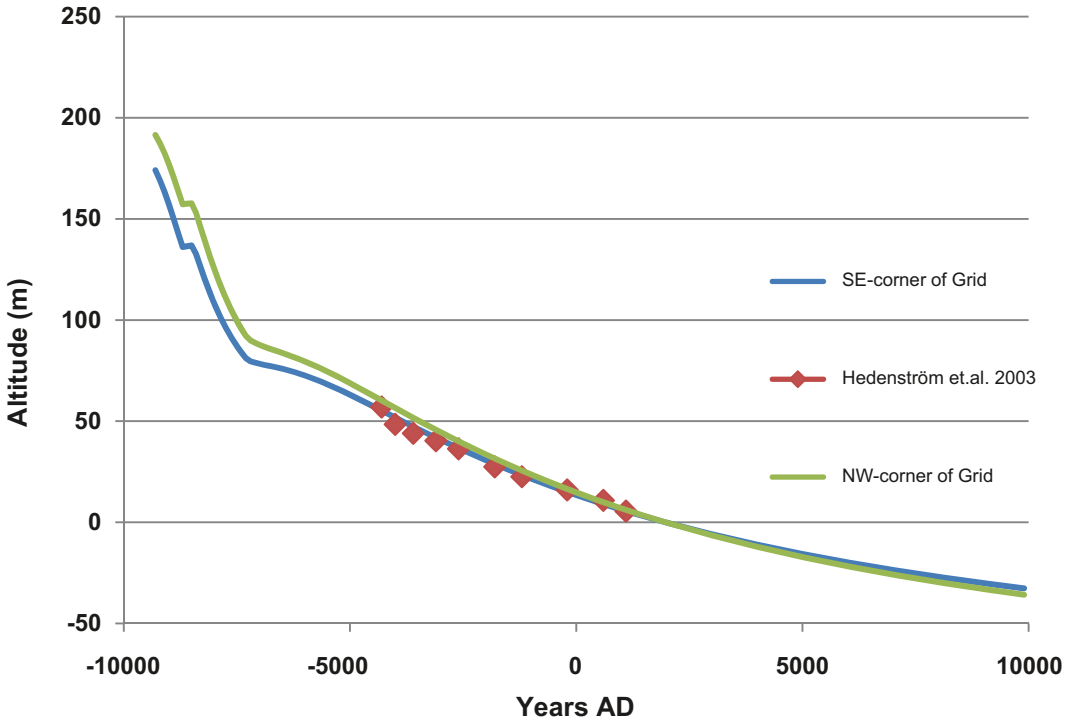

Figure 2-12. *Modelled shore displacement curves for the NW and SE corners of the Forsmark grid and shore displacement data from /Hedenström and Risberg 2003/.*

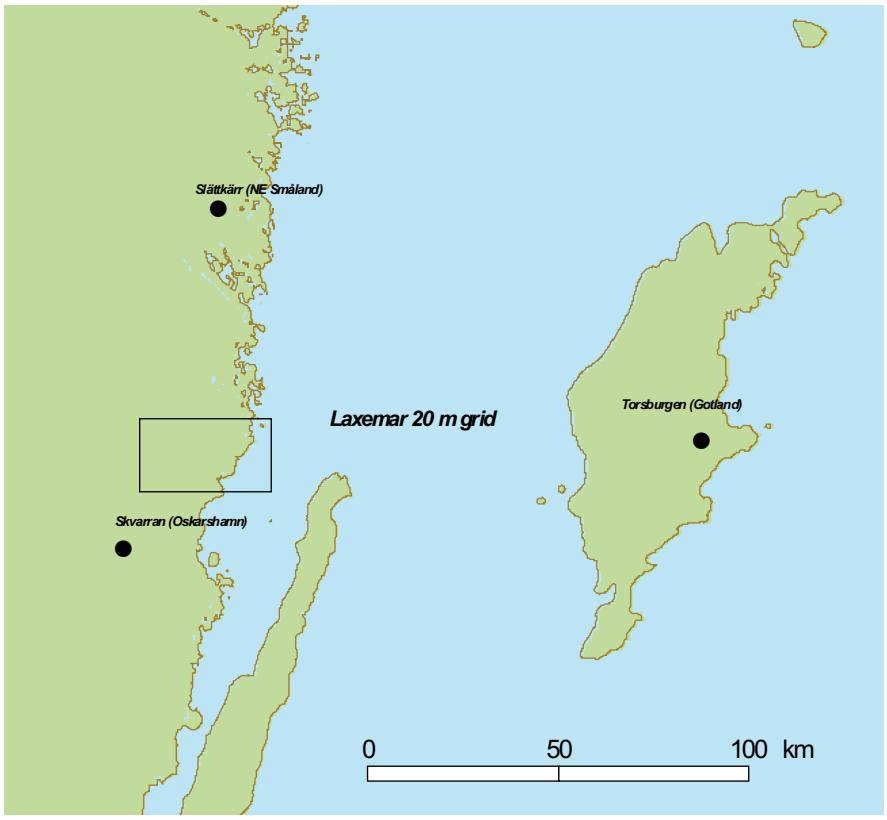

Figure 2-13. *Three sites close to Laxemar with known shore displacement equations.*

Figures 2-12 and 2-14 shows that using a single shore displacement curve for each site will generate unacceptable errors, especially early and late during the interglacial period. Consequently, the sites cannot be represented by a single shore displacement equation for each site. Using the VB-program and the method for construction of shore displacement equations from /Påsse 2001/, a shore displacement equation can be generated for a single point within the grid. As an example, parameters for the equation are presented in Table 2-4 for a point in the central part of the proposed repository sites at Forsmark and Laxemar, respectively, and Figure 2-15 displays corresponding curves.

Table 2-4. Parameters for a shore displacement equations for Forsmark /Söderbäck 2008/ and for points (X = 1631200, Y = 6699800 in RT90 2.5 gon W in Forsmark and X = 1548800, Y = 6366300 in RT90 2.5 gon W in Laxemar) in the central parts of the proposed repository sites.

Laxemar /Söderbäck (ed) 2008/	Repository site	Forsmark /Söderbäck (ed) 2008/	Repository site
163	168	270	294
2,600	3,000	7,230	7,300
24	30	93	100
11,600	11,600	11,600	11,600
400	400	1,000	1,000

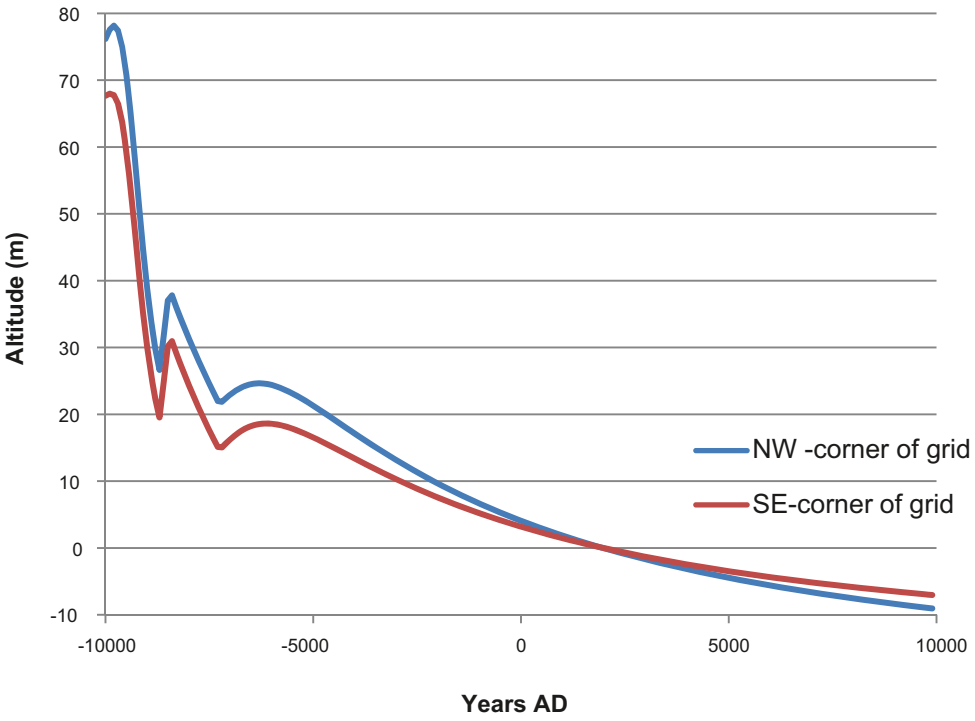

Figure 2-14. *Modelled shore displacement curves for the NW and SE corners of the Laxemar grid.*

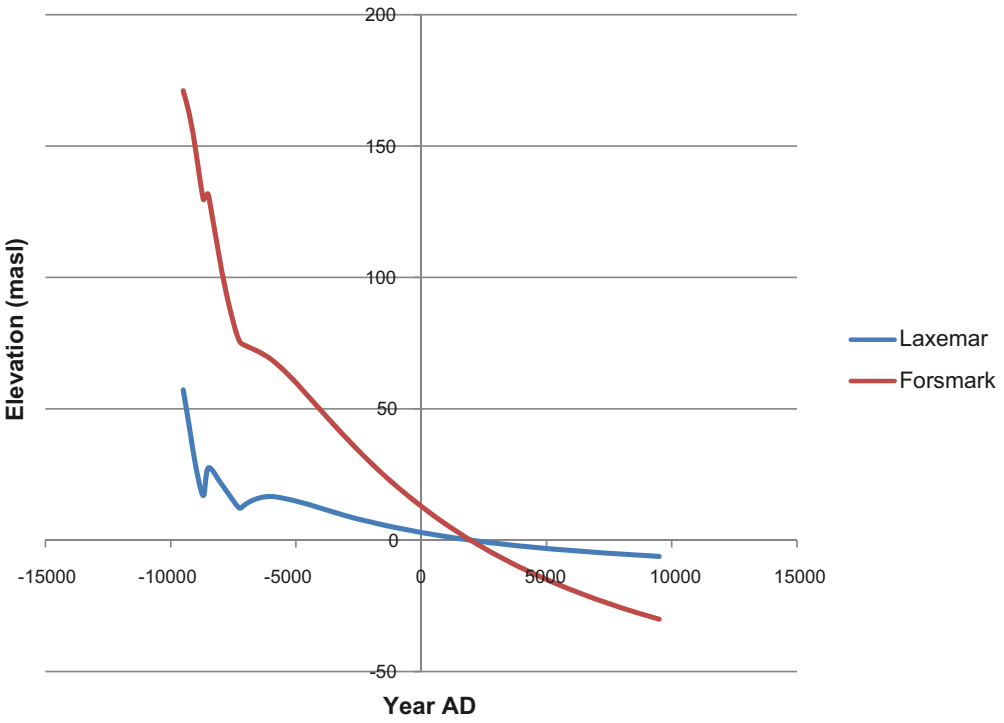

Figure 2-15. *Shore-level curves from Laxemar and Forsmark.*

Existing DEM's at Forsmark (see Figure 2-16) and Laxemar (see Figure 2-18) with a resolution of 20 meters are re-sampled to a resolution of 100 meters to fit results from the STWAVE program. The elevations in the Forsmark DEM range from –58 to 50 meters above sea level and corresponding range for Laxemar is –45 to 106 meters.

To get a view over the great change in distribution of land/sea over time, Figure 2-17 displays the distribution at four dates.

In Figure 2-14 a rapid rise in the sea level can be seen in the Laxemar area at approximately 8700 BC. This is due to the Ancylus transgression that occurred approximately 8700 BC to 7250 BC. The extension of the area affected by the transgression in Laxemar (74.4 km^2) is shown in Figure 2-20.

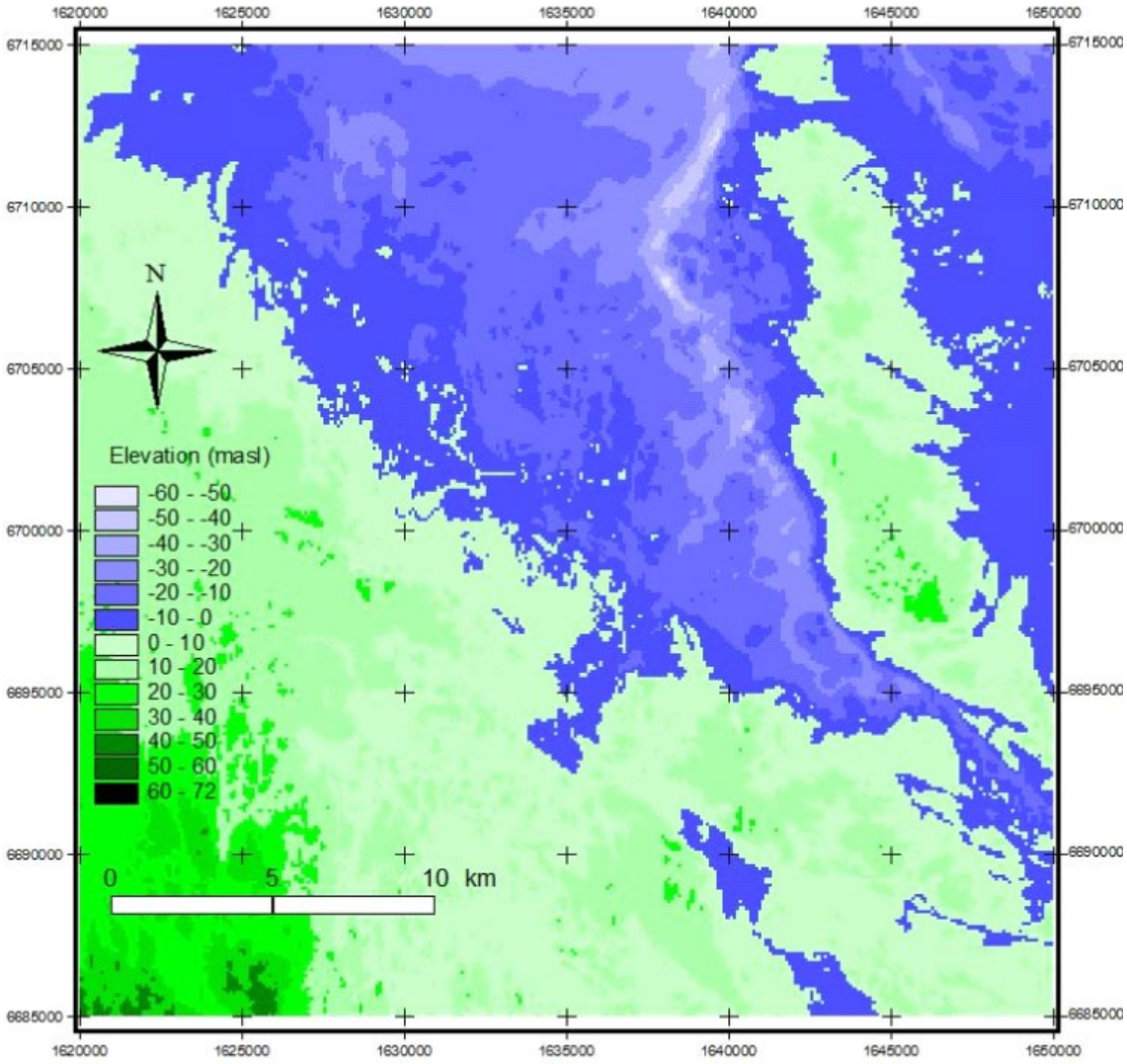

Figure 2-16. *A DEM of the Forsmark area with a resolution of 100 meters.*

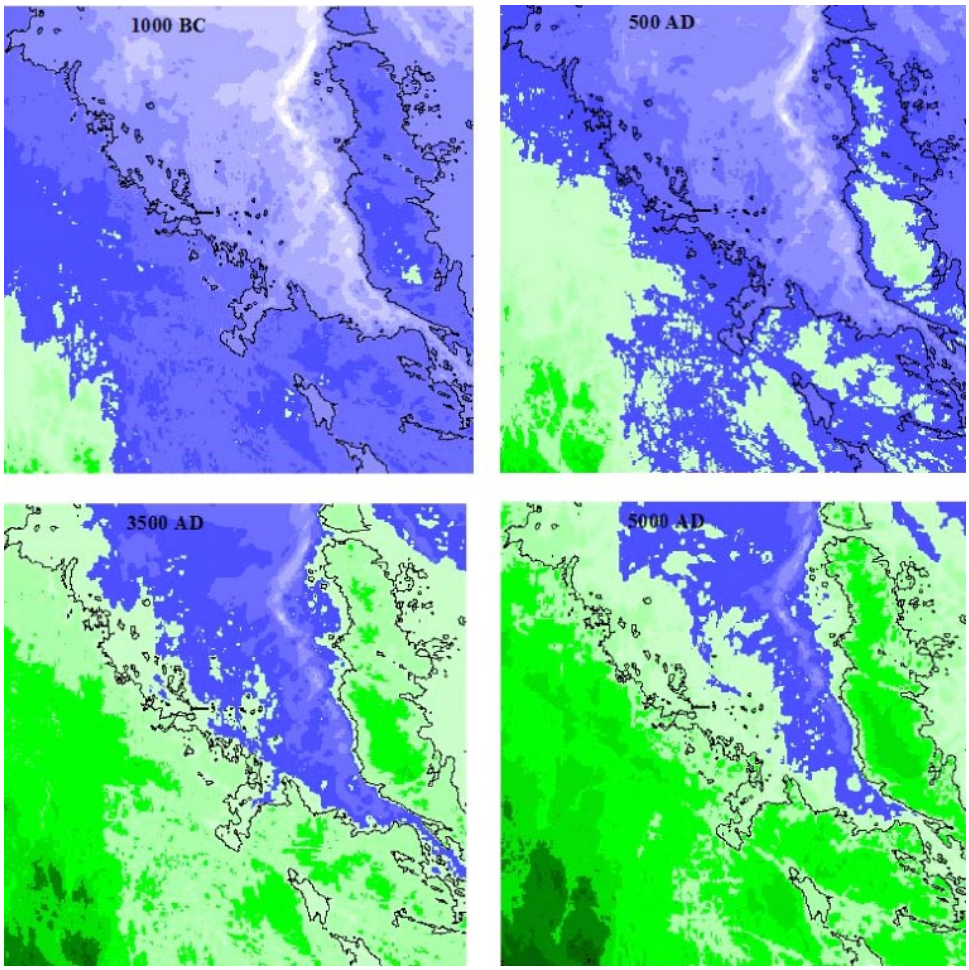

Figure 2-17. *Examples of DEMs at different dates in Forsmark. The thin black line is the shoreline at 2000 AD. The altitude legend is the same as for the DEM for 2000 AD in Figure 2-11.*

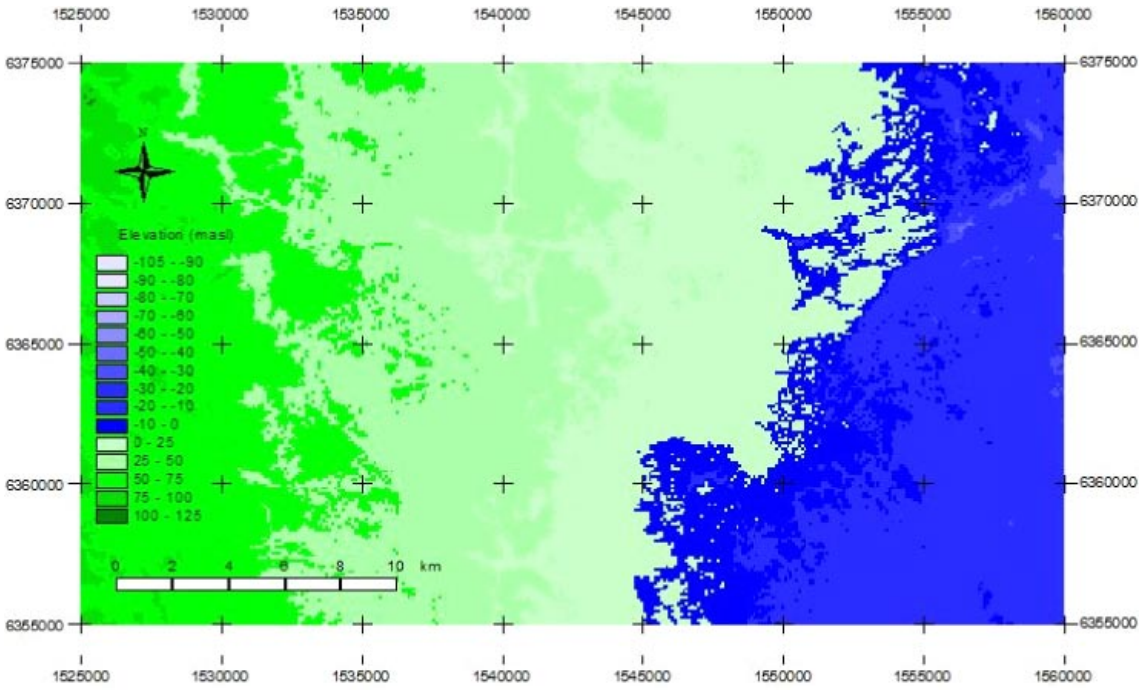

Figure 2-18. *A DEM of the Laxemar area with a resolution of 100 meters.*

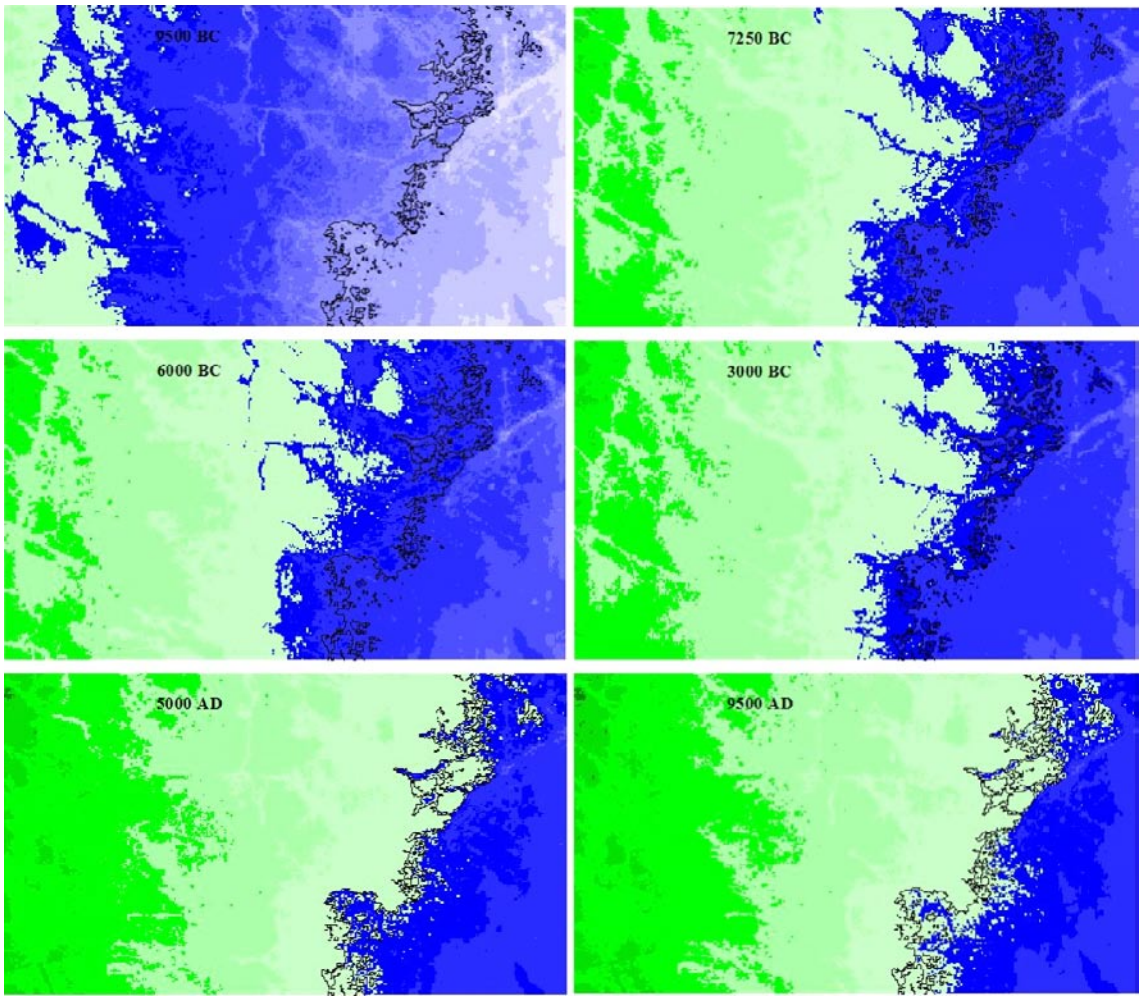

Figure 2-19. *Examples of DEM's at different dates in Laxemar. The legend is the same as for the DEM for 2000 AD in Figure 2-13. The thin black line is the shoreline at 2000 AD.*

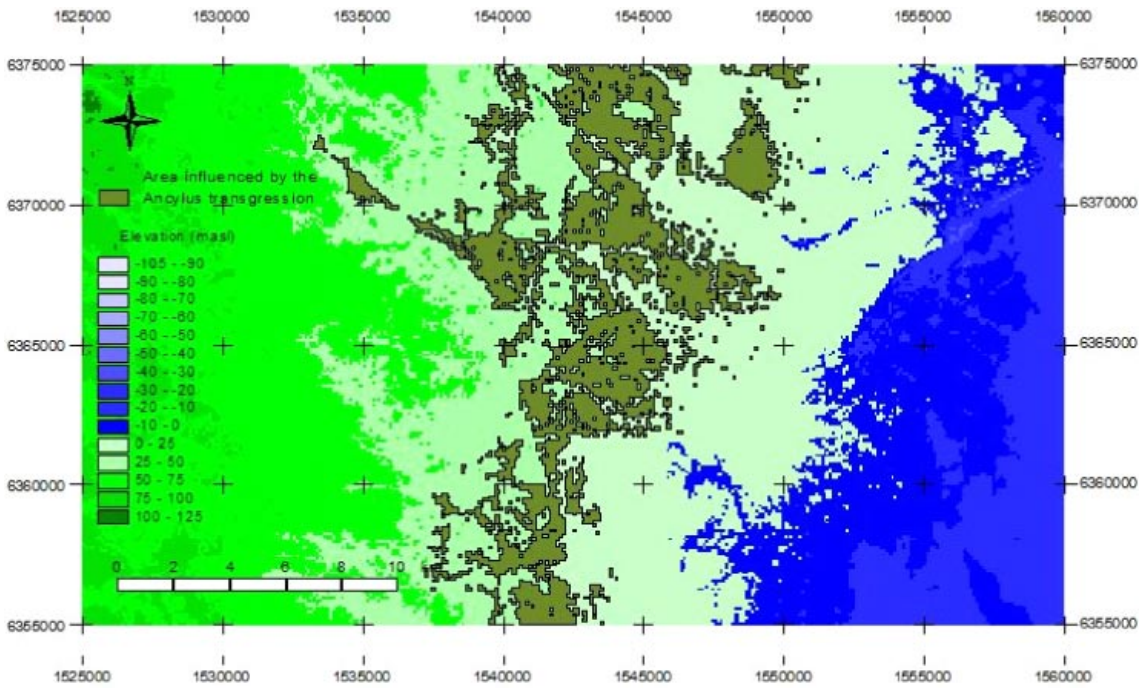

Figure 2-20. *Area in the Laxemar region affected by the Ancylus transgression.*

2.5 Choice of start values for the STWAVE-simulations

STWAVE can be performed in either a dynamic or stationary mode. In the dynamic mode the model inputs include wind data at different time steps and in the stationary mode the wind parameters are constant over time. The stationary mode is simpler to set up and run than the dynamic mode, so this is the first choice. In the stationary mode, the program simulates the wave generation, travel, and breaking along the fetch assuming that the wind duration is infinite and only the fetch limits the wave progress. Because this assumption is not always possible, it should be checked before choosing the program mode.

The fetch is limited either by the geometry of the water basin or by the extension of the weather system. If neither the fetch nor the duration is the limiting factor, the wave field is called a "Fully arisen sea" (FAS) which normally only occurs with the oceans and large lakes. At FAS, simple relationships are valid between wind speed (U), wave height (H), and wave period (T); however, if fetch or duration are limiting, there are more complicated relationships that need to be considered.

The shortest fetch for developing of FAS (FFAS) can be calculated using the following equation from /Silvester 1974/:

$$F_{FAS} = 3.19 * U_{19.5}^{1.5} \qquad \text{(Eq. 2-13)}$$

where F_{FAS} is the fetch in nautical mile and $U_{19.5}$ is the wind speed in m s^{-1} on 19.5 meters height.

To calculate the fetch in km and the wind speed at 10 meters height, equation 2-13 is converted to

$$F_{FAS} = 3.19 * \left(\frac{U_{10}}{0.5144} \right)^{1.5} * 1.852 \qquad \text{(Eq. 2-14)}$$

where U_{10} is the wind speed (m s^{-1}) at 10 meters height.

The shortest fetch for FAS is only a function of wind speed (Figure 2-21).

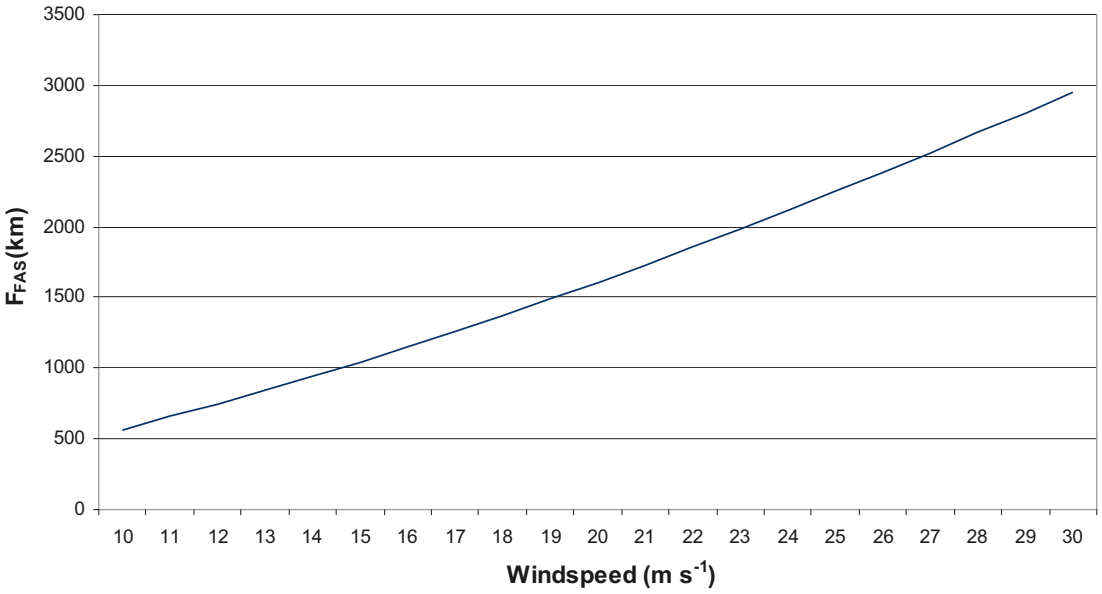

Figure 2-21. *The relationship between wind speed (m s^{-1}) and shortest fetch for generation of "Fully arisen sea" (F_{FAS}).*

For the Laxemar site, the longest fetch at present (NE) is approximately 790 km, and the easterly fetch is approximately 120 km. At the Laxemar site, at least the fetch is limited by FAS for wind speeds above approximately 14 m s^{-1} (Figure 2-21). The corresponding value for the Forsmark site is approximately 13 m s^{-1}.

Even if the fetch for higher wind speeds is only one third of what is required for FAS, this does not exclude duration as a factor that could affect wave generation. Because the minimum duration for FAS (t_{FAS}) only depends on wind speed, it can be calculated using the following equation from /Silvester 1974/:

$$t_{FAS} = 7.95 * \left(\frac{U_{10}}{0.5144} \right)^{0.5} \qquad \text{(Eq. 2-15)}$$

where t_{FAS} is the duration (h) and U_{10} is the wind speed at 10 meters height.

Figure 2-22 shows the relationship between t_{FAS} and wind speed. The minimum wind speed for duration not to be limiting is approximately 35 hours at a wind speed of 10 m s^{-1} and at least 35 hours at a wind speed of 20 m s^{-1}. High wind speeds at these latitudes are often associated with low-pressure systems moving from west to east. In these weather conditions, the winds rotate clockwise from the north toward the south ahead of the warm front and a north-westerly wind is found behind the cold front. The complete low-pressure passage takes a couple of days so it rarely has high wind speeds from the same sector for more than a day. Therefore, it is possible that also the duration can limit wave generation.

Figure 2-23 shows both the required duration for FAS for different wind speeds and the maximum durations measured at four sites (Data from Table 2-2 and Appendix). Because the measured duration strongly decreases with increasing wind speeds, and the line for t_{FAS} crosses at 15–18 m s^{-1}, only the fetch limits wave generation for wind speeds lower than approximately 18 m $s^{-1}$and either the fetch or the duration are limit wave generation at higher wind speeds.

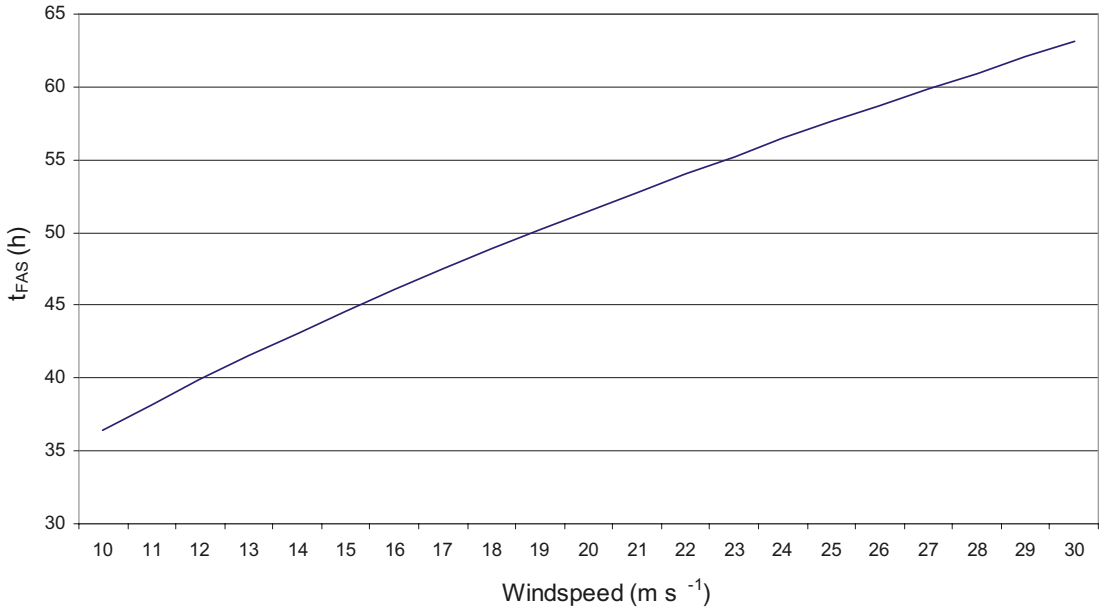

Figure 2-22. *The relationship between wind speed (m s^{-1}) and shortest duration (h) for generation of "Fully arisen sea" (t_{FAS}).*

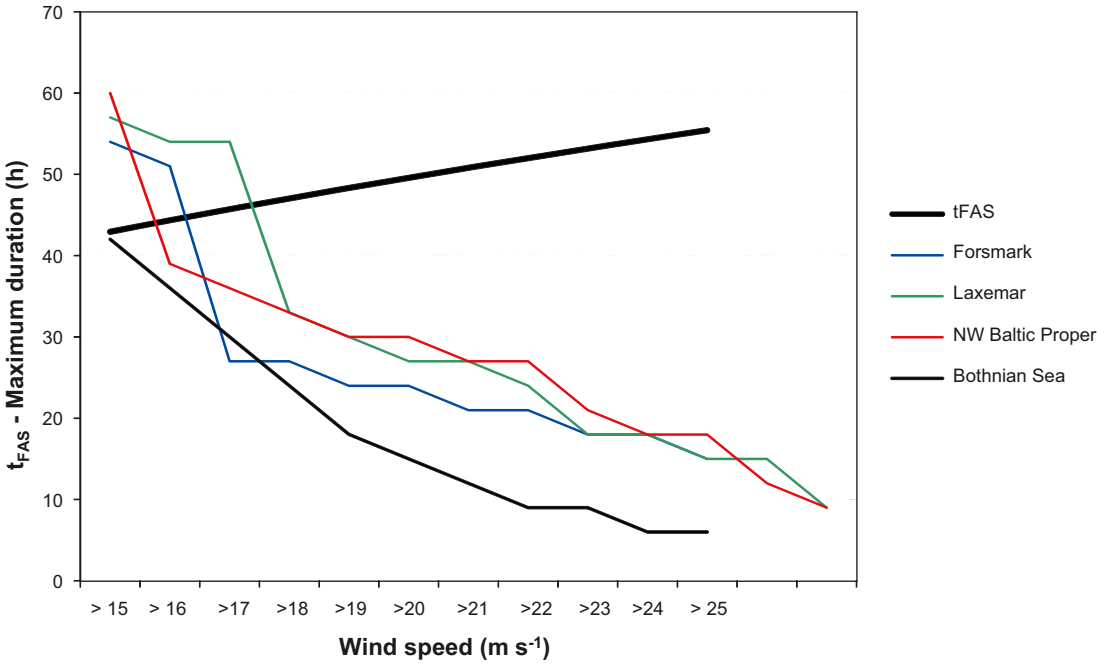

Figure 2-23. *Minimum duration for "Fully arisen sea" (FAS) and maximum duration at wind records from corrected geostrophic data. At wind speed above approximately 18 m s^{-1} the duration limits FAS.*

/Silvester 1974/ provides a method to decide which of these two parameters are the most limiting for each combination of fetch and wind speed. The method is based on a calculation of equivalent F/F_{FAS} for a dfecided t/t_{FAS}. Next, the method compares the equivalent F/F_{FAS} with the calculated F/F_{FAS} and uses the lower of the two. Figure 2-24 shows the relationship between equivalent F/F_{FAS} and t/t_{FAS}.

The relationship can be expressed as follows:

$$\left(\frac{F}{F_{FAS}}\right)_{Eq} = -8.319 + 0.8419 * \left(\frac{t}{t_{FAS}}\right) + 0.00246 * \left(\frac{t}{t_{FAS}}\right)^2 \qquad \text{(Eq. 2-16)}$$

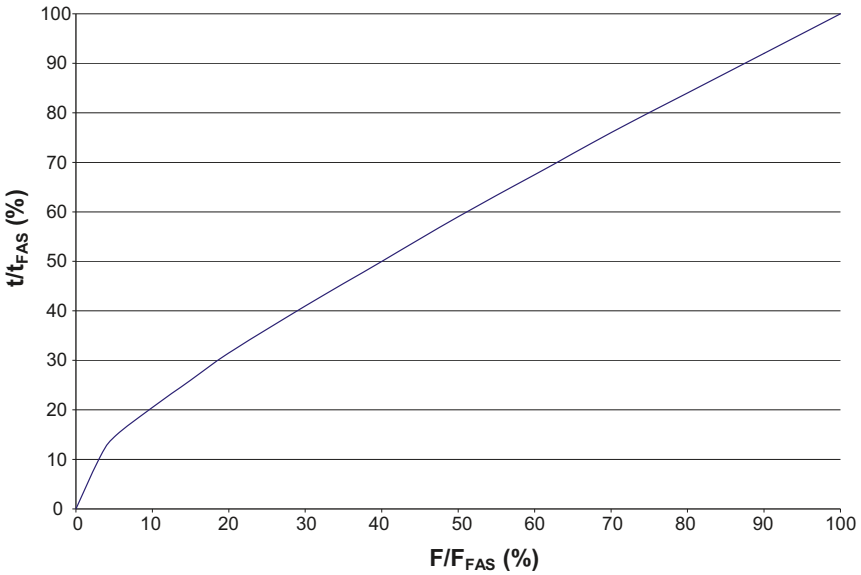

Figure 2-24. *The relationship between t/t_{FAS} and F/F_{FAS}.*

The parameter t_{FAS} can be calculated with equation 2-15 and t can be determined using geostrophic wind data (Appendix) and then the quotient t/t_{FAS} can be calculated. The table shows the maximum duration at the Forsmark site for different wind speeds during the period 1990–2004. The appendix also lists corresponding data for the following sites; central Bothnian Bay, central Bothnian Sea, Forsmark, NW Baltic Proper, and Laxemar.

Table 2-5 shows an example of calculation of limiting parameter. The example is for the Laxemar site for north-easterly wind (fetch = 790 km). For wind speeds lower than 14 m s^{-1} neither the fetch nor the duration is limiting and for higher wind speeds the fetch limits the wave generation ($F/FFAS < F/FFAS_{Eq.}$).

Example 2 (Table 2-5) is for the Forsmark site with wind data from the Forsmark site and a wind direction from NE (a dominant direction for wave action in Öregrundsgrepen, especially in the future (AD 2000–AD 6500)). In spite of shorter durations at the Forsmark site compared to northern Baltic Proper, at this site the fetch is also the limiting factor ($F/FFAS < F/FFAS_{Eq.}$).

For some extreme combinations of fetch and durations, it is possible that the duration can be the limiting factor. The modelled geostrophic wind speeds at central Bothnian Sea are considerably lower than the other five sites and the northern fetch for Forsmark at BC 9000 was long, approximately 950 km. The calculation of the limiting factor for this combination shows that the duration is the limiting factor for wind speeds higher than 20 m s^{-1}. When using all three geostrophic wind data sites that affects the wave generation along the fetch, the fetch and the duration are found to limit wave generation to the same degree.

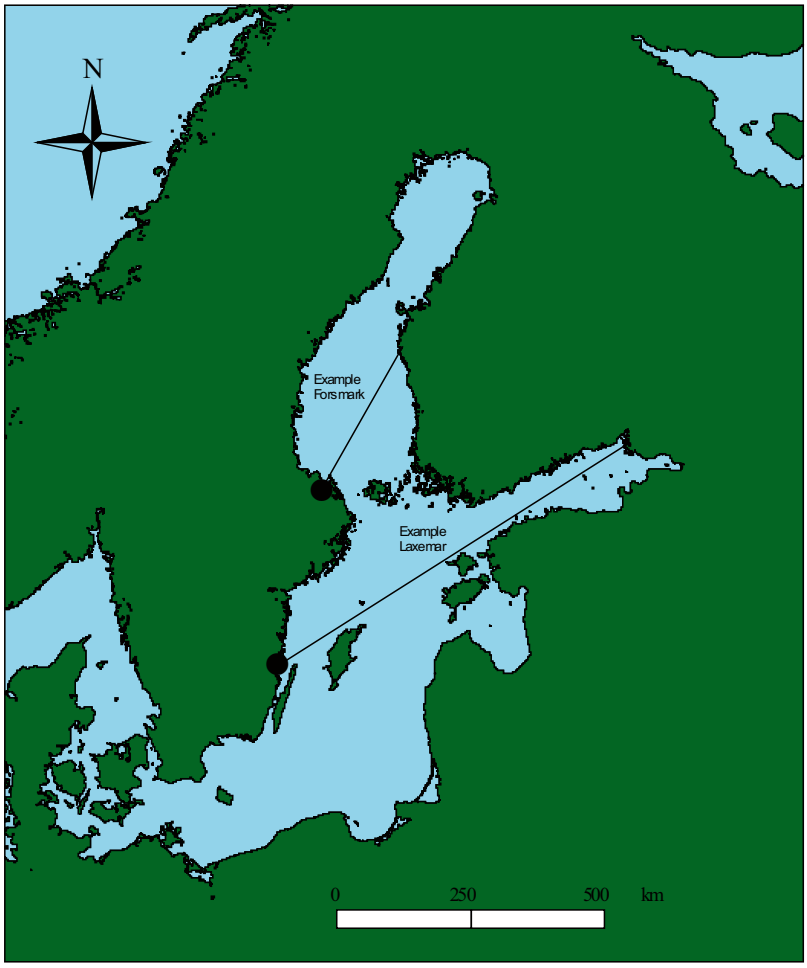

Figure 2-25. *Two examples of fetches for which the limiting factor for wave generation are calculated (see Table 2-4 and 2-5).*

Table 2-5. Calculation of limiting parameter for the Laxemar site for north-westerly winds (fetch = 790 km). Values for duration t (h) are from appendix. Wind speed (U_{10}) is in m s^{-1} and FFAS in km.

U_{10}	FFAS	F/FFAS	tFAS	t	t/tFas	F/FFAS eq
10	506	1.56	35.05	75	2.14	2.84
11	584	1.35	36.76	72	1.96	2.51
12	666	1.19	38.40	69	1.80	2.22
13	751	1.05	39.97	66	1.65	1.98
14	839	0.94	41.47	66	1.59	1.88
15	930	0.85	42.93	66	1.54	1.79
16	1,025	0.77	44.34	66	1.49	1.72
17	1,122	0.70	45.70	45	0.98	0.98
18	1,223	0.65	47.03	39	0.83	0.78
19	1,326	0.60	48.32	36	0.75	0.68
20	1,432	0.55	49.57	30	0.61	0.52
21	1,541	0.51	50.80	30	0.59	0.50
22	1,652	0.48	51.99	27	0.52	0.42
23	1,766	0.45	53.16	27	0.51	0.41
24	1,883	0.42	54.30	27	0.50	0.40
25	2,002	0.39	55.42	27	0.49	0.39

Table 2-6. Calculation of limiting parameter for the Forsmark site for northeasterly winds (fetch = 290 km). Values for duration t (h) are from appendix. The unit for wind speed (U10) is m s^{-1} and for FFAS is km, respectively.

U_{10}	FFAS	F/FFAS	tFAS	t	t/tFas	F/FFAS eq.
10	506	0.57	35.05	72	2.05	2.68
11	584	0.50	36.76	69	1.88	2.36
12	666	0.44	38.40	69	1.80	2.22
13	751	0.39	39.97	63	1.58	1.86
14	839	0.35	41.47	60	1.45	1.65
15	930	0.31	42.93	54	1.26	1.37
16	1,025	0.28	44.34	51	1.15	1.21
17	1,122	0.26	45.70	27	0.59	0.50
18	1,223	0.24	47.03	27	0.57	0.48
19	1,326	0.22	48.32	24	0.50	0.40
20	1,432	0.20	49.57	24	0.48	0.38
21	1,541	0.19	50.80	21	0.41	0.31
22	1,652	0.18	51.99	21	0.40	0.30
23	1,766	0.16	53.16	21	0.40	0.29
24	1,883	0.15	54.30	18	0.33	0.22
25	2,002	0.14	55.42	15	0.27	0.16

After analysing the tests of limiting factors for wave generation, it was determined that the static mode in the STWAVE program could be effectively used. During extreme combinations of low durations and long fetches, the choice of program mode will give some overestimation of the resuspension processes.

As already mentioned, the STWAVE models will be used for a classification of sea bottoms into three classes:

1. Erosion bottoms,
2. Transport bottoms, and
3. Accumulation bottoms.

In erosion bottoms, fine-grained particles will never accumulate because the time between two resuspension occasions is shorter than the time for a fine-grained particle to settle. In practice, this is impossible to model so the definition is generalized to "A bottom where fine-grained particles is settled less than one month or during a period with ice coverage". This means that the resuspension frequency should be at least 12 times per year. This can be calculated using data from Figure 2-23 and the Appendix. The figure shows that the minimum duration for tFAS at different wind speeds and using data from the Appendix gives the frequencies for different limiting combination of wind speeds and durations (Table 2-7).

The table shows that the wind speed used for classification of erosion bottoms varies between sites; on average it is approximately 10–11 m s^{-1}. In order to be conservative (not an overestimation of the extension of the erosion bottoms), a wind speed of 10 m s^{-1} was chosen.

The accumulation bottom is defined as a bottom where no resuspension occurs during a time step. The bathymetry is constant at each time step so the fetches are also constant; only the wind speeds vary. The goal is to determine the highest wind speed that occurs at all sites during a 500-year time step based on data from a 15-year period. Table 2-1 suggests that the limiting wind speed could be approximately 25–28 m s^{-1} and using the conservative approach, the choice will be 25 m s^{-1}. This conservatism implies that the extensions of the accumulation bottoms will be overestimated.

In chapter 4, the rationale for limiting values for both erosion and accumulation bottoms (10 and 25 m s^{-1}, respectively) will be discussed.

Finally, transport bottoms are defined as all bottoms not classified as erosion or accumulation bottoms. The conservative choice of limiting wind speed values for erosion and accumulation bottoms means that the transport bottoms are overestimated near the erosion bottoms and underestimated near the accumulation bottoms.

Table 2-7. Frequency (occasions per year) of limiting combinations of wind speed and duration for six sites in the Baltic Sea.

	Wind speed (m s^{-1}) – *Duration (h)*		
Site	**10 – *36***	**12 – *39***	**14 – *42***
Forsmark	45	11	4
Bothnian Bay	52	14	3
Bothnian Sea	23	5	1
Laxemar	40	8	1
NW Baltic Proper	66	17	3
N Baltic Proper	78	23	5

2.6 STWAVE models

Because the depth Cartesian grid used in STWAVE has a non-standard format it was generated using the SMS program. The interpolation method in SMS used to transform point data to a grid is unknown, but it seems to be IDW. To preserve the quality of the Baltic Sea DEM (500 meters resolution) in the transformation to the STWAVE DEM (2,000 meters resolution), the following method is used:

1. The Baltic Sea DEM is converted to points in ArcGis,
2. A new DEM with 2,000 meters resolution is interpolated in ArcGis with Ordinary Kriging method,
3. This new DEM in ESRI grid format is converted to points in ESRI shape-format,
4. Fields holding X- and Y-coordinates in RT90 2.5 gon W datum are added to the shape-file,
5. The shape-file attribute table is exported to text format, and
6. This text-file is imported to SMS and used for interpolation to a SMS Cartesian grid with exactly the same extension and resolution as an ESRI 2,000 meter grid.

This method preserves the values from the Kriging interpolation in ArcGis irrespective of interpolation method used in SMS since one point is placed exactly in the middle of each cell in the SMS grid.

Each cell in the SMS-grid must be declared either as land or ocean and is not permitted to have isolated ocean cells. Doing this manually is extremely time-consuming. Because at least hundred grids will be generated in this study, it was necessary to develop an automatic method for this classification. This was done using the following method:

1. The ESRI-grid in 2,000 meters resolution was reclassified into two classes; lower or higher than –1 meter. The choice of –1 meter as classification limit is because the STWAVE is sensitive to cells that vary between wet or dry. To assure that no such cells exist, only cells with water depth exceeding 1 meter were classified as ocean.
2. The reclassified grid was converted to polygons in shape-format without performing weeding (the raster structure is preserved in the polygon edges).
3. In this polygon shape there can be a number of isolated ocean areas within the land mass that will be classified as land and a number of islands within the large ocean polygon that will also be classified as land. The large ocean polygon was selected. The “switch selection tool” was used to select all polygons except the large ocean polygon. These polygons were merged into one single polygon using the “union tool” and the result is a polygon shape with only two polygons, land and ocean.
4. This polygon shape-file was imported to SMS and used to classify the SMS grid into land/ocean.

The method for classification of the grid cells into land/ocean was the same as for the coarse grids.

The grids in SMS were orientated parallel with the major wave directions and the STWAVE models are called “half-plane models”. This means that the waves cannot refract more than 90 degrees clockwise or counter-clockwise from the grid orientation. Therefore, if the high-resolution areas are affected by waves spread from more than 180 degrees, two coarse-grids are necessary to provide input data for the high-resolution grids. This is the case at early time steps at both sites.

Figures 2-26 and 2-27 shows the extensions of the coarse grids for Forsmark and Laxemar, respectively. At early time-steps for Laxemar, the northern coarse grid must be extended to cover the whole Gulf of Bothnia.

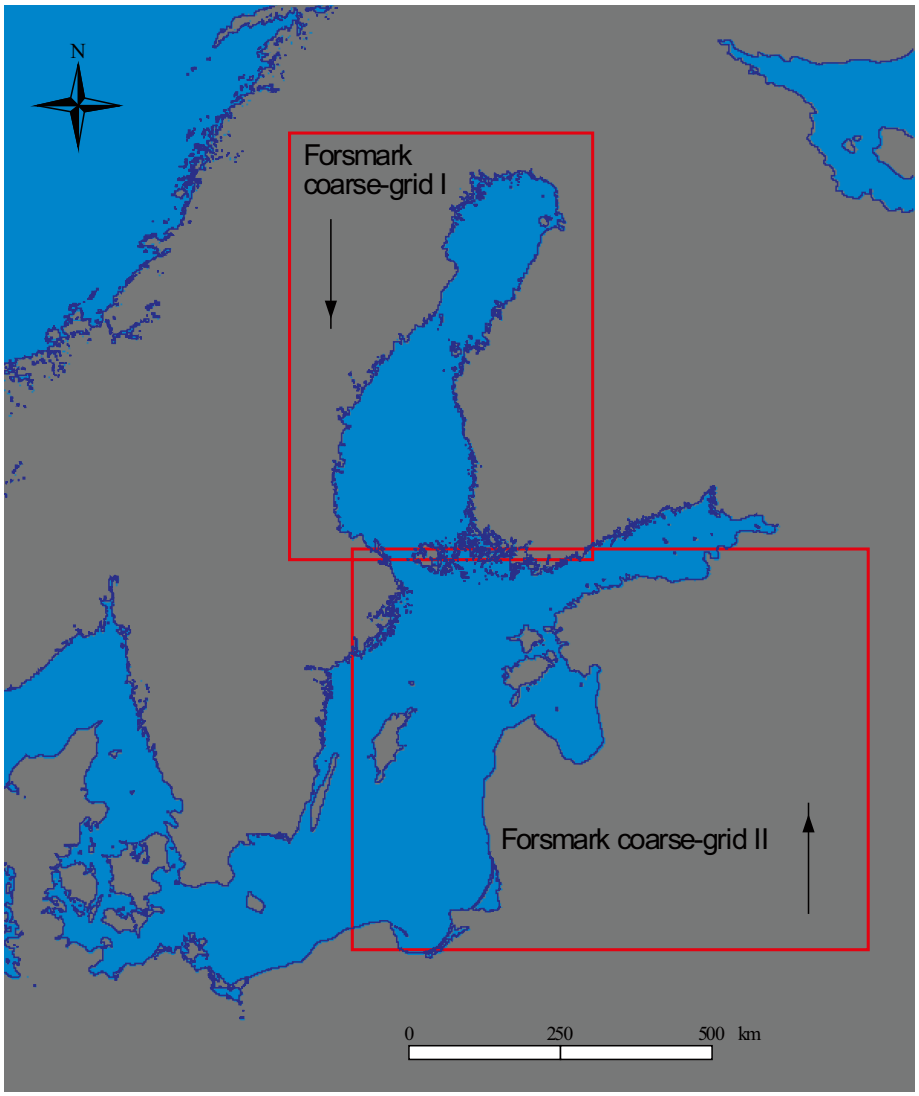

Figure 2-26. *Extension of the coarse grids used in SMS for the Forsmark simulation.*

2.7 The resuspension model

The resuspension model is based on a semi-empirical relationship devised by /Komar and Miller 1973/:

$$\frac{\rho u_t^2}{(\rho_s - \rho) g\, MRG} = 0.21\pi \left(\frac{d_0}{MRG}\right)^{1/2} \qquad \text{(Eq. 2-17)}$$

where $u_t = \frac{\pi d_0}{T}$ (Eq. 2-18)

$$d_0 = \frac{H}{\sinh\left(\frac{2\pi h}{L}\right)} \qquad \text{(Eq. 2-19)}$$

where ρ is the density of the water, ρ_0 is the density of the sediment grains, u_t is the required near-bottom horizontal orbital velocity for motion of sediment grains, g is the acceleration of gravity, MRG is the grain size, d_0 is the near-bottom horizontal major diameter of the elliptical water particle motion, T is the wave period, H is the wave height, h is the water depth, and L is the wave length.

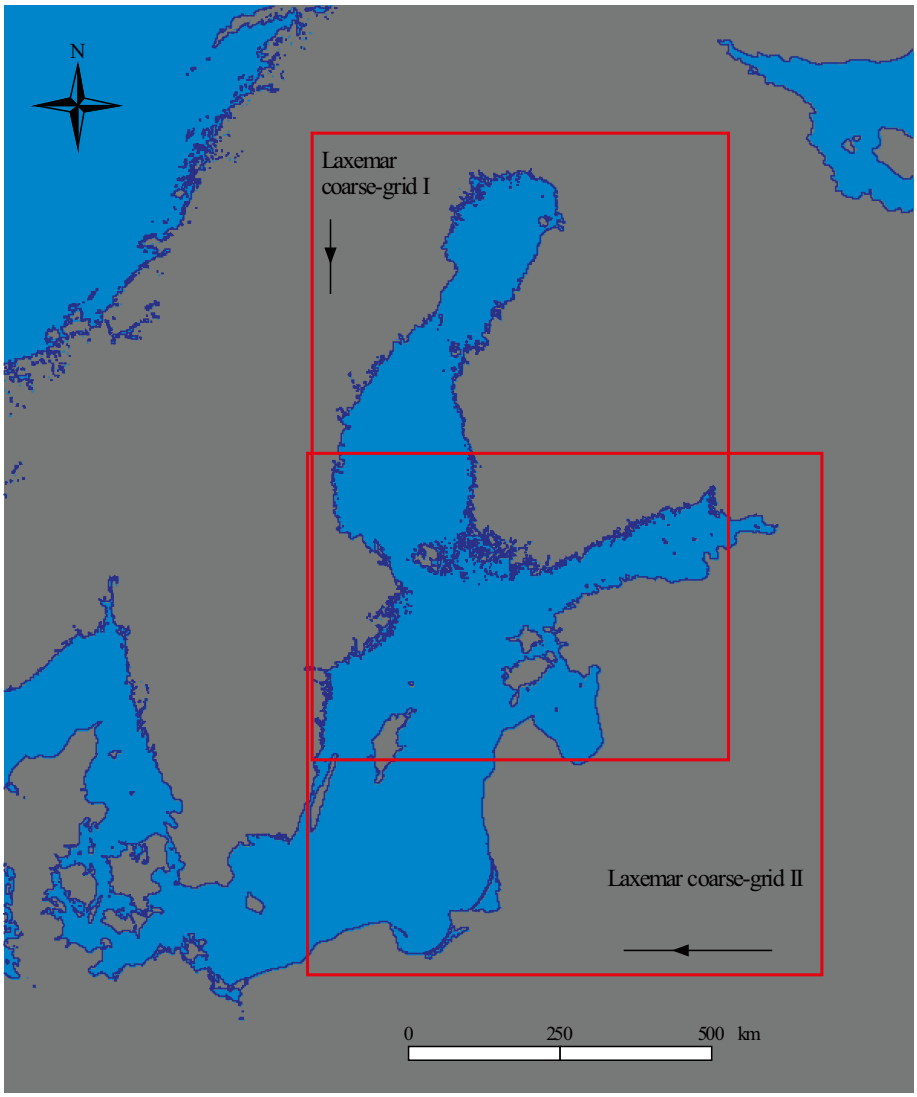

Figure 2-27. *Extension of the coarse grids used in SMS for the Laxemar simulation.*

With known values of water depth (h), wave height (H), and wave period (T), it is possible to calculate maximum resuspendable grain size (MRG). The equation is restricted to grain sizes less than about 0.5 mm (medium sand and finer).

2.8 Processing STWAVE model results in a Visual Basic Program

The STWAVE program is run for the period 9500 BC to 9500 AD with a time step of 500 years. At each time step both 10 and 25 m s^{-1} situations are simulated; for each wind speed, five wind directions are simulated. The wave spectra for each combination of wind speed and wind direction are saved for an overlapping cell of the coarse and fine grids. These wave spectra were used as input to STWAVE simulations with the fine grids.

The STWAVE fine-grid simulations give results for wave height, wave period and wave directions for each combination of wind speed and wind direction in SMS grid format. These results were exported in generic text format.

A Visual Basic program was generated to link SMS program results with ArcGis, where all post processing was performed. The Visual Basic program executes the following tasks:

(i) Reads the five generic text files (wave height and period for five wind directions) for one wind speed and stores these data in 2D arrays.

(ii) Finds the maximum wave height for each cell among the five arrays and finds the wave period value associated to that maximum wave height.

(iii) Reads the water depth generic text file and stores values in a 2D array.

(iv) Calculates the maximum resuspendable grain size for each cell in the grid using equations 2-17 to 2-19 and data for wave height, wave period, and water depth. Since the grain size (MRG) exists on both sides of equation 2-17, an equation solver is included in the VB-program.

(v) Converts the grid from SMS format to ESRI ASCII grid format by mirroring the SMS grid over the either the Y-axis or the X-axis depending on the SMS-grid orientation.

The two ASCII-grids were imported to ArcGis and converted to ESRI grid format. The grids were reclassified into two classes using the MRG-value. The two reclassified grids were combined into a single grid with five classes:

1 Land,
2 Accumulation bottom,
3 Transport bottom,
4 Erosion bottom, and
5 No Data.

The “No Data” class is grid cells classified as ocean without any MRG-values situated at water depth shallower than one meter. The reason for the lack of MRG-values at these cells is described above.

2.9 Validations of the wave and resuspension models

The only output variables from the STWAVE simulations used as input to the resuspension model are wave height and wave period, so these are the variables to be validated.

Since June 2006, the Swedish meteorological and hydrological institute (SMHI) has operated a wave buoy in the Bothnian Sea (Finngrundet, 60° 54’ N, 18° 37’ E). Using weather data from Örskär (S. Bothnian Sea) three different combinations of wind speeds and wind directions has been simulated with the STWAVE model. These results can be compared to measured wave buoy data (see Table 2-8). Situations with the same wind directions during the previous 24 hours were chosen and the maximum wind speed during that period was simulated. The modelled wave heights were compared with the maximum measured wave heights during or shortly after that period.

Although the STWAVE model gives excellent results, this validation does not really test the wave refraction component of the model since the Finngrundet wave buoy floats on deep water.

The resuspension model is calibrated using the marine geology data from the Forsmark area. The borders between accumulation bottoms and transport bottoms are usually defined to be between postglacial fine-grained sediments and postglacial coarse-grained sediments or against bedrock/till/

Table 2-8. Comparison between measured wave heights at Finngrundet wave buoy and modelled wave heights at the same position. The measured wave heights are given as significant wave heights ($H_{1/3}$) and are converted to H_{Max} by multiplying it by 1.66 /Silvester 1974/. Wind speed in m s^{-1} and wave heights in m.

Date	Wind speed	Measured H	Modelled H
2006-10-31	29	8.1	7.9
2006-11-02	17	4.2	4.3
2006-05-06	12	1.8	1.7

glacial clay. However, occurrence of fine-grained postglacial sediments does not always indicate an accumulation bottom since a late switch from accumulative to erosion environment cannot be observed by the methods used in the geological survey. Normally, an erosion environment can be proven if there are thin layers of sand on top of the clay sediments, but this occurrence is normally not shown in the geological map. On the other hand, a late switch between erosion to accumulation environment will only provide a thin layer of fine-grained particles on top of coarser material. These characteristics are not shown in the map or in the sediment sample.

To avoid using sites with late change in sedimentation environments, only sites with either thick (> 1 m) or no occurrence of postglacial fine-grained sediments are used in the calibration. This sediment thickness rule (> 1m) makes it impossible to use the marine geological map in the calibration since this map only shows the surficial sediment type and not the sediment profile. Therefore, only data from the sonar surveys are used in the calibration. To use only modelled data with no late switch in sedimentation environment, only sites where the model shows no change in environment during the last three time steps (1,500 years) are used.

Moreover, since the water depth is an important factor in the MRG calculations, only sites (grid cells) where the water depths in the SMS grid are approximately the same as the measured water depths presented in the geological data set are used for calibration.

The geological survey data were classified into erosion or accumulation sediment: postglacial clays or silts were classified as accumulation sediment and all other sediment types were classified as erosion sediments (postglacial sand is an accumulation sediment but is not situated at an accumulation environment for fine-grained particles).

The MRG-value that will be used for classification into Accumulation/No accumulation was calculated by minimizing the number of wrongly classified cells (postglacial clay classified as postglacial sand or postglacial sand classified as postglacial clay). A MRG-value of 0.27 mm (fine sand) was found to give the lowest error and approximately 84% of the cells used for calibration were correctly classified.

The resuspension model is validated using data from the geological survey at the Laxemar site. The results for the AD 2000 simulation in raster format and five classes (Accumulation, Transport, Erosion, Land and No Data) were converted to points.

The marine geological map exists in two versions, both in polygon shape format. One map shows the geological unit at approximately 0.5 m depth and the other map shows the thin unit on top if it differs from the first map. In this validation, a combination of the two is used; the thin unit map where it exists and the unit on 0.5 meters depth at all other sites.

The model results were linked to the geological map and a table with fields for model class and geological units were generated. The total number of points in the validation is 3,274. Unfortunately, the distributions of different geological units in the Laxemar area are skewed with strong domination erosion or transport bottoms. Table 2-9 shows the results of the validation.

Table 2-9. Results from validation of the resuspension model using a MRG-value of 0.27 mm for the Laxemar area. The columns are the modelled classes and the rows the marine geological units. The values are the number of points for each combination of modelled bottom class and marine geological unit. Numbers marked in italic are wrongly classified points and in bold correctly classified points. MRG = Maximum Resuspendable Grain size.

Modelled unit	Mapped unit Bedrock	Glacial clay	Till	Postglacial sand gravel	Postglacial fine sand	Postglacial clay
Accumulation	107	6		46	99	23
Transport	1,718	198	5	637	215	
Erosion	189	9		21	1	

Correctly classified points are 92% of total number of points. The most seriously wrongly classifications are bedrock points classified as accumulation bottoms (107 points). Possible causes for this miss-classification are discussed in chapter 4. In addition to the high share of correctly classified points, it is also positive that the model correctly classifies all the postglacial clay points. Moreover, the validation also shows that the extensions of accumulation bottoms are overestimated, a finding that is expected when using conservative approach to choose limits.

The validation of how the resuspension model predicts extension of erosion bottoms are more complex since erosion bottoms can appear as all geological units except postglacial clay.

3 Results

The outcome of the modelling is time series of classified maps in raster format with classes for different bottom types. Figure 3-1 shows the change in extension of different bottom types over time for the Forsmark site. The shore displacement process can be seen as increasing land area (green line) with time for the first island appearing at approximately 3500 BC. At the beginning of the period, the bottom is solely of accumulation type since wave base is higher than the shallowest bottom at this time. As the area becomes shallower over time, some accumulation bottoms become situated higher than the wave base and these bottoms are transferred to transport bottoms (the shallow effect). At the same time, the shallow process in the wave generation areas also causes shortening of the fetch, lowering the energies of the waves that affects the resuspension process (the fetch effect).

The shallow parts of the sea area between the deep sea and the Öregrundsgrepen also causes some wave energy to be lost because of bottom friction or wave breaking. This decrease in wave energy causes waves entering the sea border of the site decrease in height over time (the wave energy filter effect). Therefore, the shallow effect causes the areas of accumulation bottoms to decrease over time (transfers to transport bottoms and later to erosion bottoms), whereas the fetch effect and the wave energy effect works in the opposite direction. The balance between these three effects change over time and results in the change in extension of bottom types (Figure 3-1).

The shallow effect dominated between 9000 BC and 3500 BC, whereas the combination of wave energy filter effect and fetch effect dominates after 1500 BC. During the intermediate period (3500 BC–1500 BC), the effects are balanced.

Figures 3-2 to 3-4 shows examples of extensions of different bottom types at the Forsmark site on three dates, 2000 AD, 3000 BC (when the minimum accumulation bottom area occurred), and 500 BC (when the accumulation bottom has a local maximum).

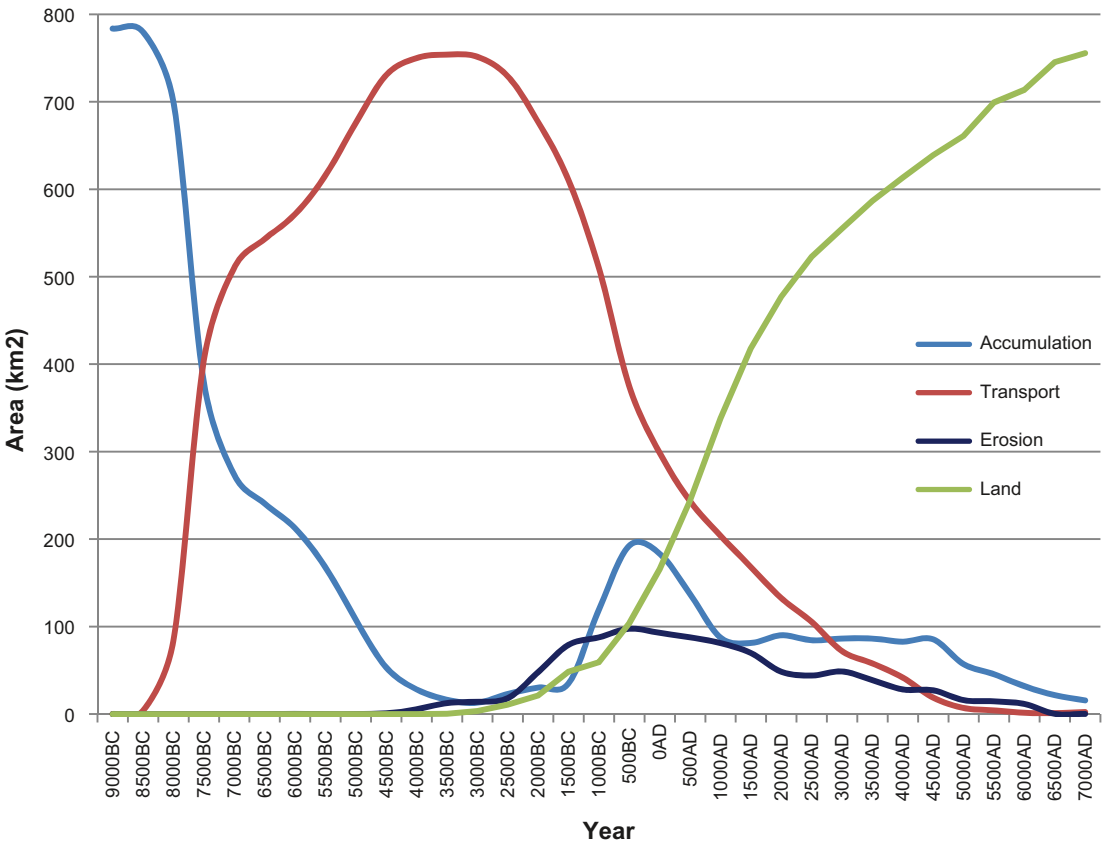

Figure 3-1. *Change in area extensions over time in three bottom types at the Forsmark site.*

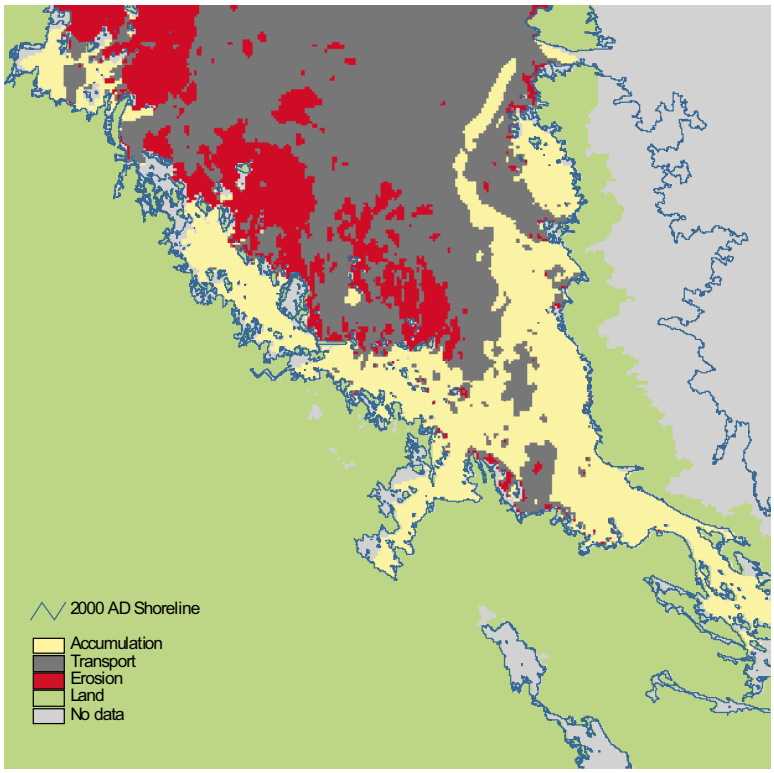

Figure 3-2. *Extensions of modelled different bottom types in Forsmark at 2000 AD. The large area in the NE corner of the map is excluded from the analysis due to patches with unknown water depth values but this has no importance for the implementation of the results while it is situated outside the site domain.*

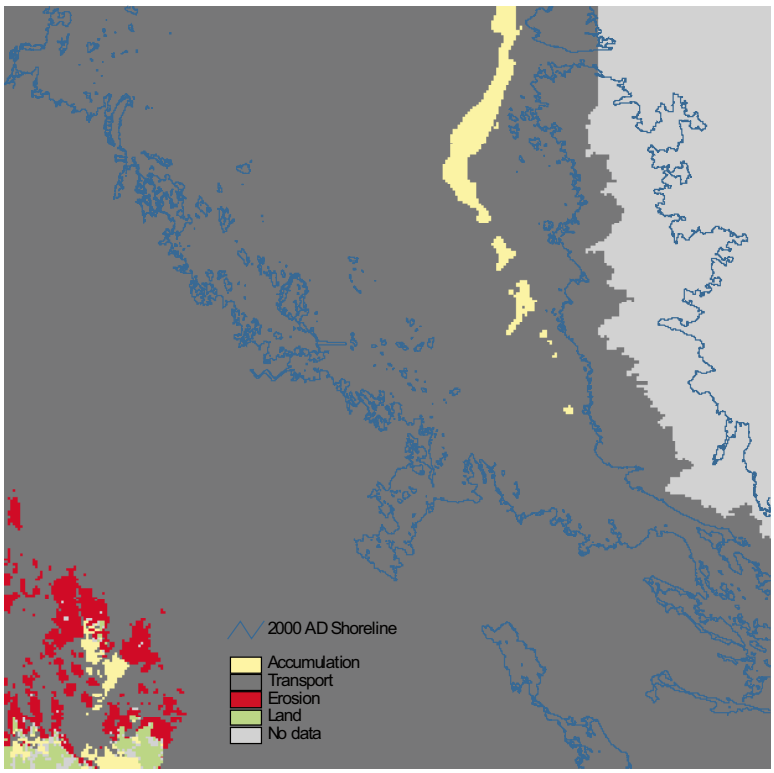

Figure 3-3. *Extensions of modelled different bottom types in Forsmark at 3000 BC. The thin blue line is the shoreline at 2000 AD.*

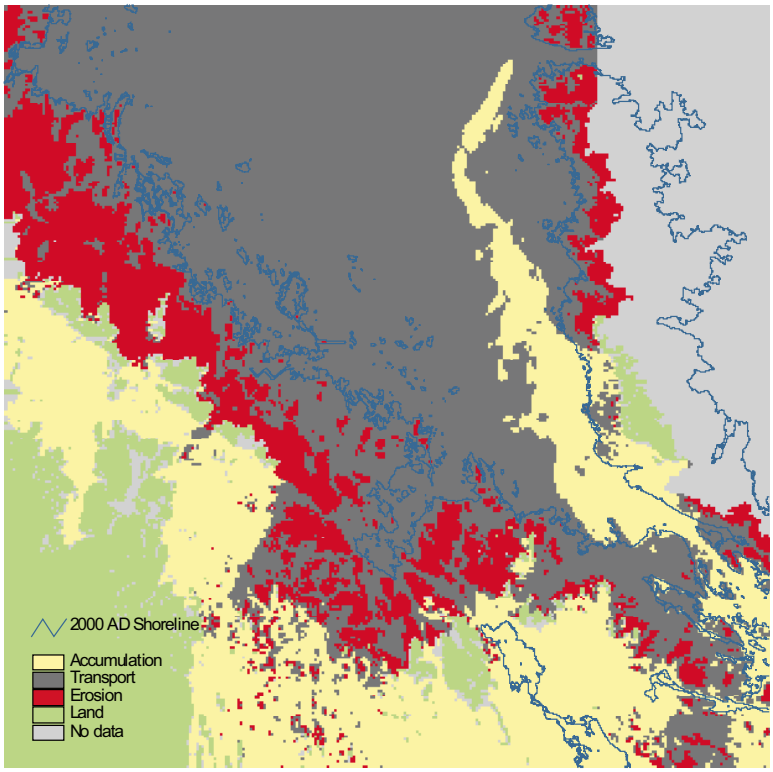

Figure 3-4. *Extensions of modelled different bottom types in Forsmark at 500 BC. The thin blue line is the shoreline at 2000 AD.*

These raw results (the results before the classification) can be used to understand how existing quaternary geological features (e.g. the basin of Lake Bolundsfjärden) in the Forsmark area have been affected by accumulation/transport processes over time (see Figure 3-5 for location of Lake Bolundsfjärden).

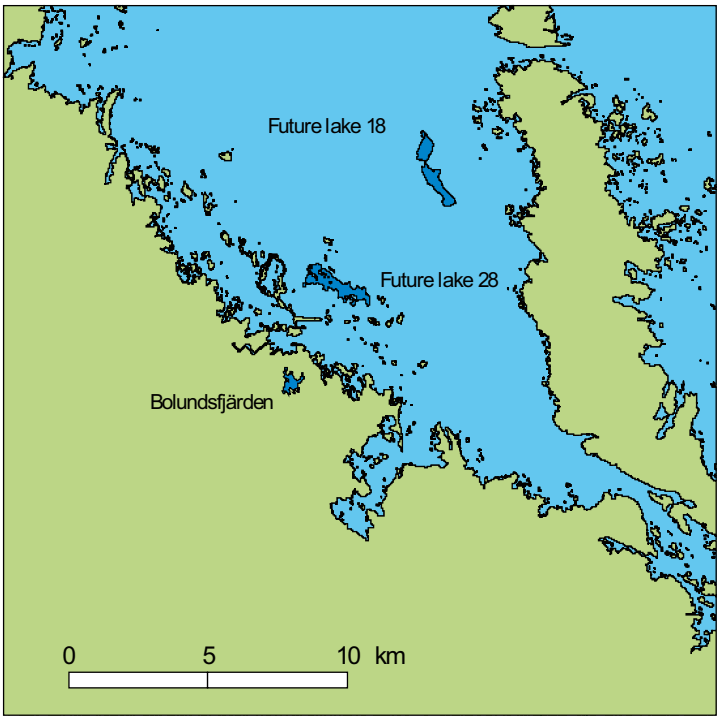

Figure 3-5. *Location of a lake in an isolation phase (Bolundsfjärden) and two future lakes that will have different characteristics (water volumes and maximum water depths).*

For each time step, the minimum, average, and maximum MRG-values within the Lake Bolundsfjärden polygon are extracted from the simulation of 25 m s^{-1} wind speed. These extracted values are displayed in a MRG-time diagram that also shows the MRG threshold value of 0.27 mm. If all three values are situated below the threshold, values reveal the whole area as an accumulation sediment environment, whereas values above the threshold indicate that the area is eroding. If the maximum value is above the threshold while the minimum value is below, a focusing process is in progress (the fine-grained particles are transported from erosion sub-area to the accumulation sub-area).

The MRG-time diagram for Bolundsfjärden (Figure 3-6) shows that after deglaciation, a period of 2500 years accumulation occurred. This was followed by a long period with erosion that probably eroded the former accumulated particles and this was followed by a short period with accumulation before the lake was isolated. During this short final phase, only a minor volume of sediment could have been accumulated and at approximately 1000 AD a focusing process occurred (part of the lake erosion environment and the other part with accumulation) with a concentration of the small volume to the deepest part of the future lake. In /Hedenström 2004/, a figure is presented that shows the thickness of different geologic strata along a profile in the lake. Postglacial fine-grained sediments settled in marine/brackish environment (gyttja clay) generally occur in a thin stratum (< 10 cm) with the thickest accumulation of approximately 70 cm situated in the deepest part of the lake basin.

An additional example deals with the future lakes 18 and 28 in Forsmark, which will have different physical characteristics (Table 3-1). The two lakes will be of approximately the same area, but Lake 28 will be an extreme shallow lake while Lake 18 will be a deep lake compared to existing lakes in the region (see Figure 3-7).

Table 3-1. Future lake characteristics and number of survey points (%) in SGU marine geological survey of different surficial sediment types in Lake 18 and 28, respectively. Lake 18 is dominated by accumulated fine-grained sediments and Lake 28 shows postglacial fine sand within a transition from an environment with erosion to accumulation.

	Altitude (m)	Max depth (m)	Isolation (Year AD)	Clay/Silt (%)	Fine sand (%)
Lake 18	–34.3	6.2	10,500	62	0
Lake 28	–14.0	1.4	4,600	0	38

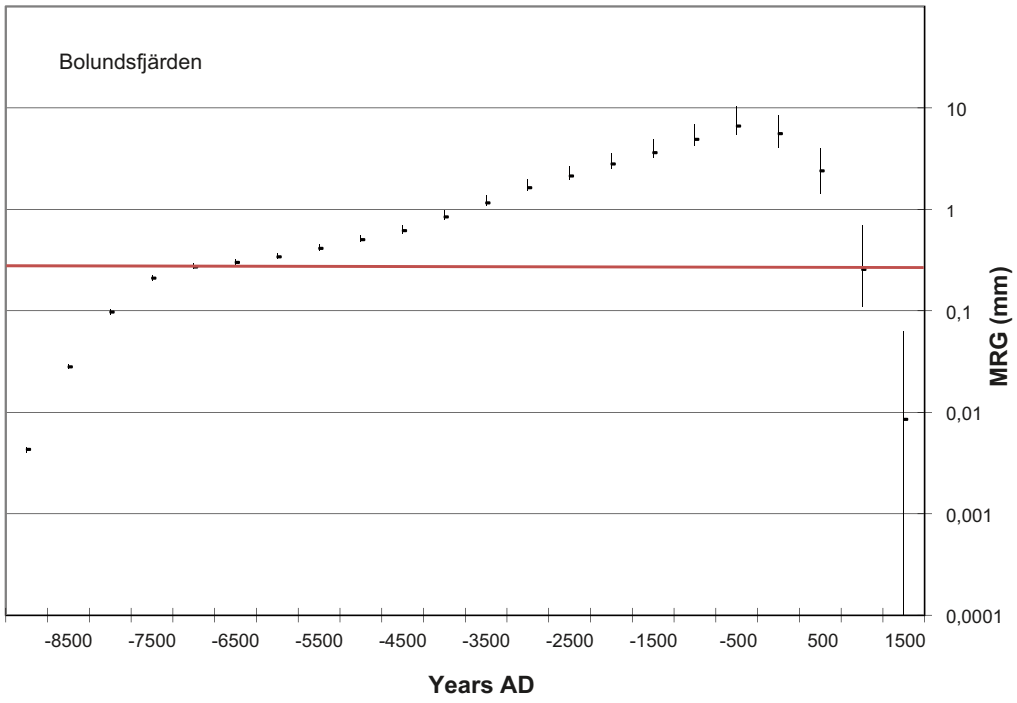

Figure 3-6. *A MRG – time diagram (min – average – max) for the Lake Bolundsfjärden (see Figure 3-5). MRG = Maximum Resuspendable Grain size.*

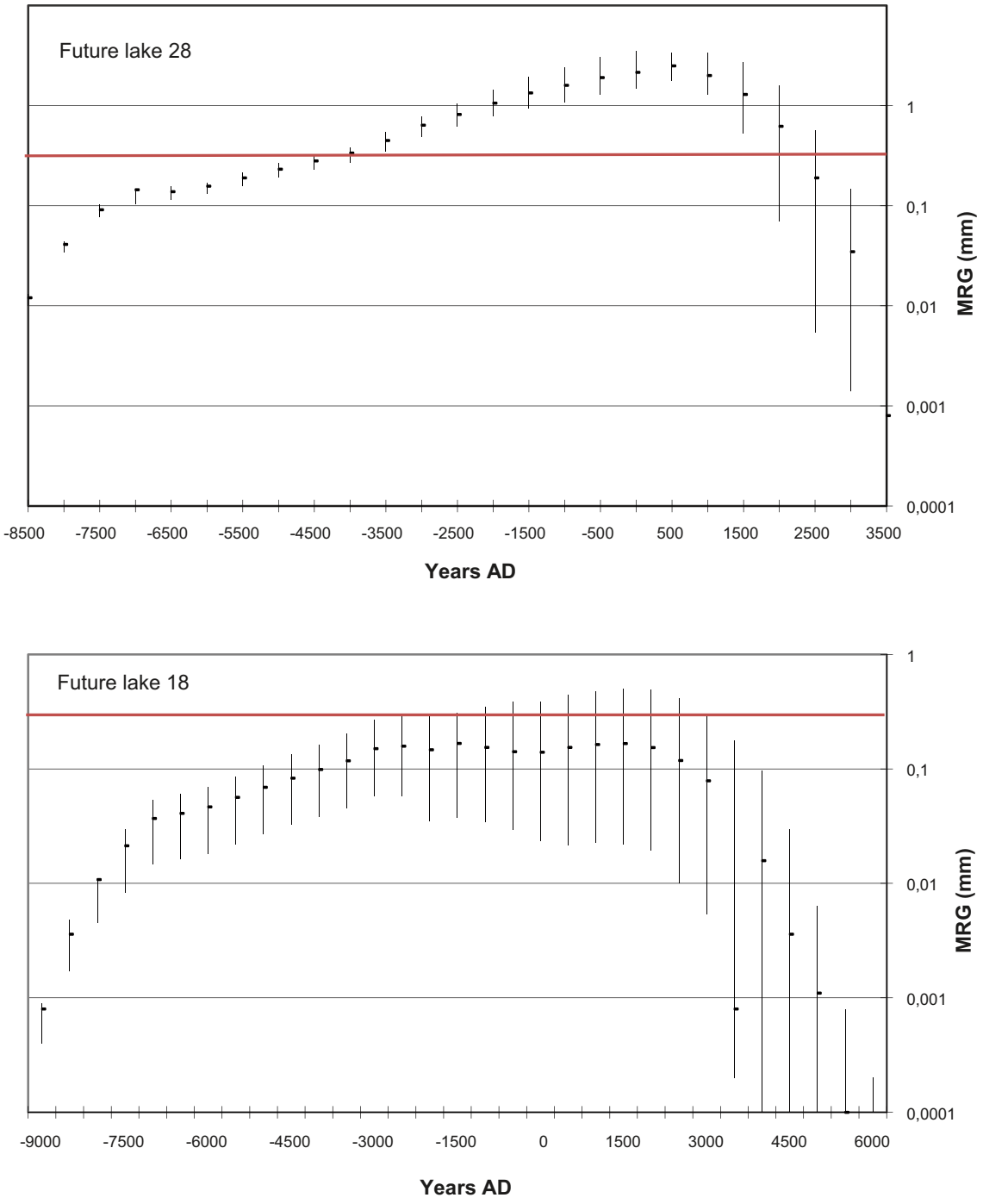

Figure 3-7. *A MRG – time diagram (min – average – max) for the future Lake 18 and Lake 28 (see Figure 3-5). MRG = Maximum Resuspendable Grain size.*

For the two future lakes, the overall patterns of the MRG-time diagrams are similar, a bell-shaped pattern with low MRG-values after deglaciation and a period before lake isolation and a local maximum in between. The differences in MRG between the lakes are mainly the bandwidths (the difference between minimum and maximum MRG at each time step) and the level of the local maximum. The broad bandwidth for Lake 18 is due to the large differences in water depth among the pixels in the lake and the difference in local maximum is due to different open sea exposure that depends on different altitudes. The higher located Lake 28 (the lake surface will be at –14.0 masl) will be affected by waves generated in a much deeper and larger sea compared to Lake 18 (–34.3 masl).

The basin that will be Lake 28 has been exposed to erosion for 6,000 years and only a part of the basin has had a recent period of accumulation. No fine-grained sediments are found in the basin at the marine geological survey /Elhammer and Sandqvist 2005a/ (Table 3-1), but proportionately large extent of fine sand indicates a transition from erosion to accumulation is in progress.

The maximum MRG-values for Lake 18 shows erosion for only part of the future lake basin, so the other part of the basin will have accumulation throughout the whole interglacial period in a marine basin (9000 BC–10500 AD), and in a lake that forms in the basin. Approximately 62% of the bottom area is presently covered by postglacial clay, in some parts of the lake are covered with a thick strata (> 4 m) /Elhammer and Sanqvist 2005a/.

Figure 3-8 shows a map with bedrock lineaments. The red point is a location where four lineaments cross, a possible discharge point for deep groundwater. Figure 3-9 shows the MRG-time diagram for that point. If a radionuclide is transported in the groundwater before 5500 BC, it would be bound to fine-grained particles at the sea bottom and possibly be trapped there. After 5500 BC, the location change from an accumulation bottom to an erosion bottom and the contaminated particle will be resuspended and transported to the water mass. Radionuclides entering the sea bottom with ground water between 5500 BC and 2000 AD will not be trapped but immediately be transported to the water mass, while nuclides entering after 2000 AD will be trapped and later (after 3000 AD) be part of the quaternary deposit on land.

Figures 3-10 to 3-15 shows how the simulation results can be used to analyze sediment phenomenon at the Laxemar site. Figure 3-10 shows the change in area extensions of different bottom types at the Laxemar site (corresponding figure for the Forsmark site is Figure 3-1). Over the whole period (9500 BC–9000 AD), the only major change is that transport bottoms are transferred into land, whereas accumulation and erosion bottoms are almost constant over time (note the great difference between the two sites). Due to the rapid shore displacement immediately after deglaciation (Figure 2-14), more than half of the transport bottoms at Laxemar are transferred into land during the first 3000 years. Although the shore displacement is as fast in Forsmark, no such effects are evident there, because the first land in the Forsmark domain does not show up not until c. 3000 BC. Between c. 6000 BC and 3000 BC, the changes in areas of different bottom types in Forsmark are subtle.

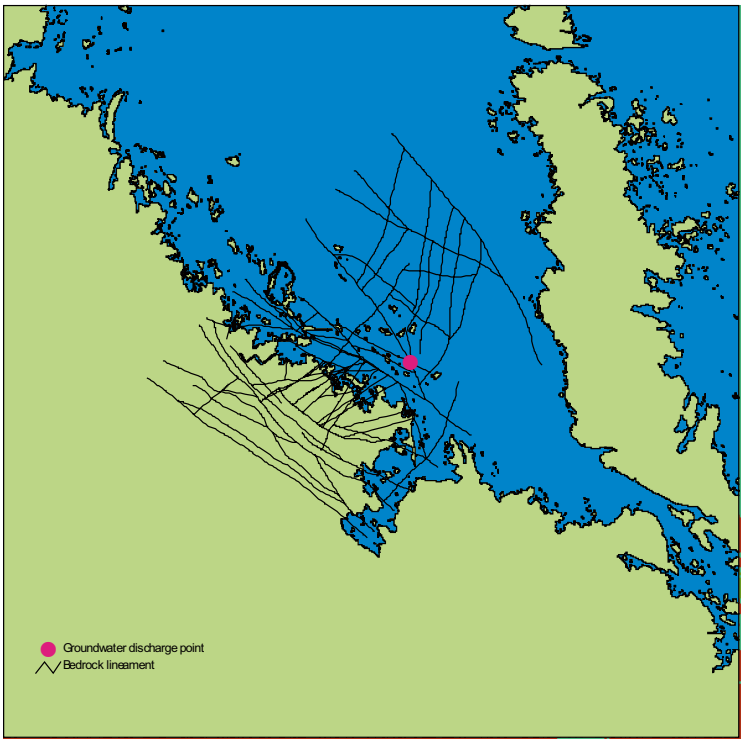

Figure 3-8. *A possible discharge point for deep groundwater situated in the cross of four bedrock lineaments. The MRG-time diagram for the point is shown in Figure 3-9. MRG = Maximum Resuspendable Grain size.*

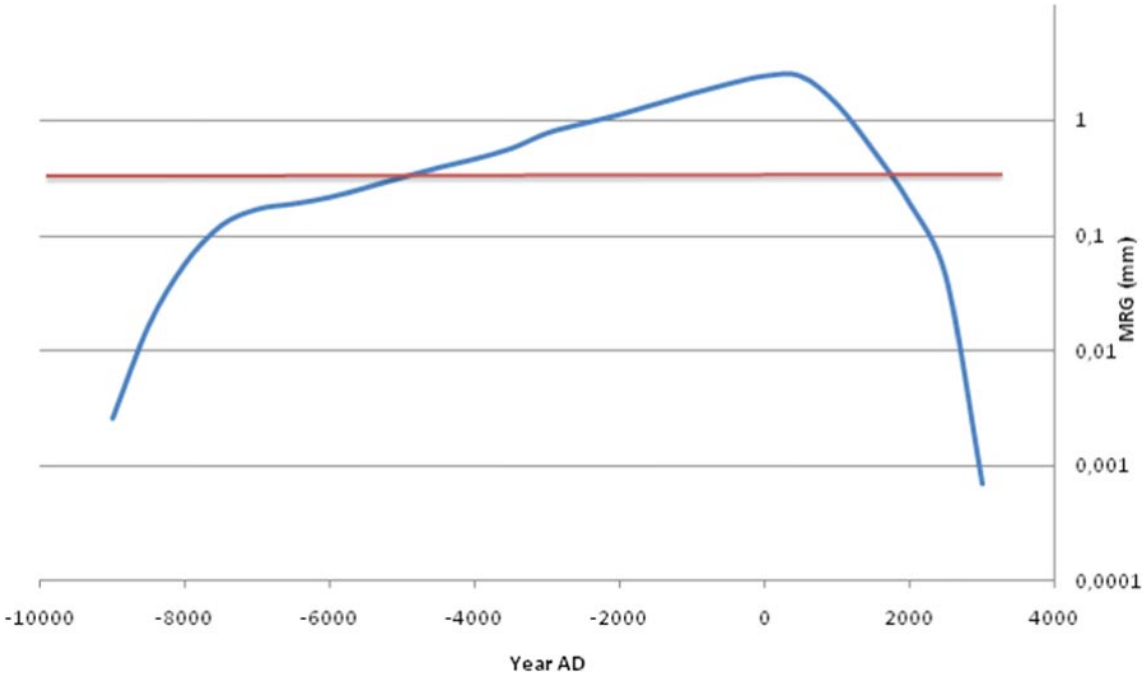

Figure 3-9. *A MRG-time diagram for the bedrock lineament cross shown in Figure 3-8. MRG = Maximum Resuspendable Grain size.*

The Figure 3-10 also displays the effects of the Ancylus transgression (c. 8700–7300 BP) (see Figure 2-20). Approximately 20 km^2 former lands were once more submerged and mainly transferred to transport bottoms.

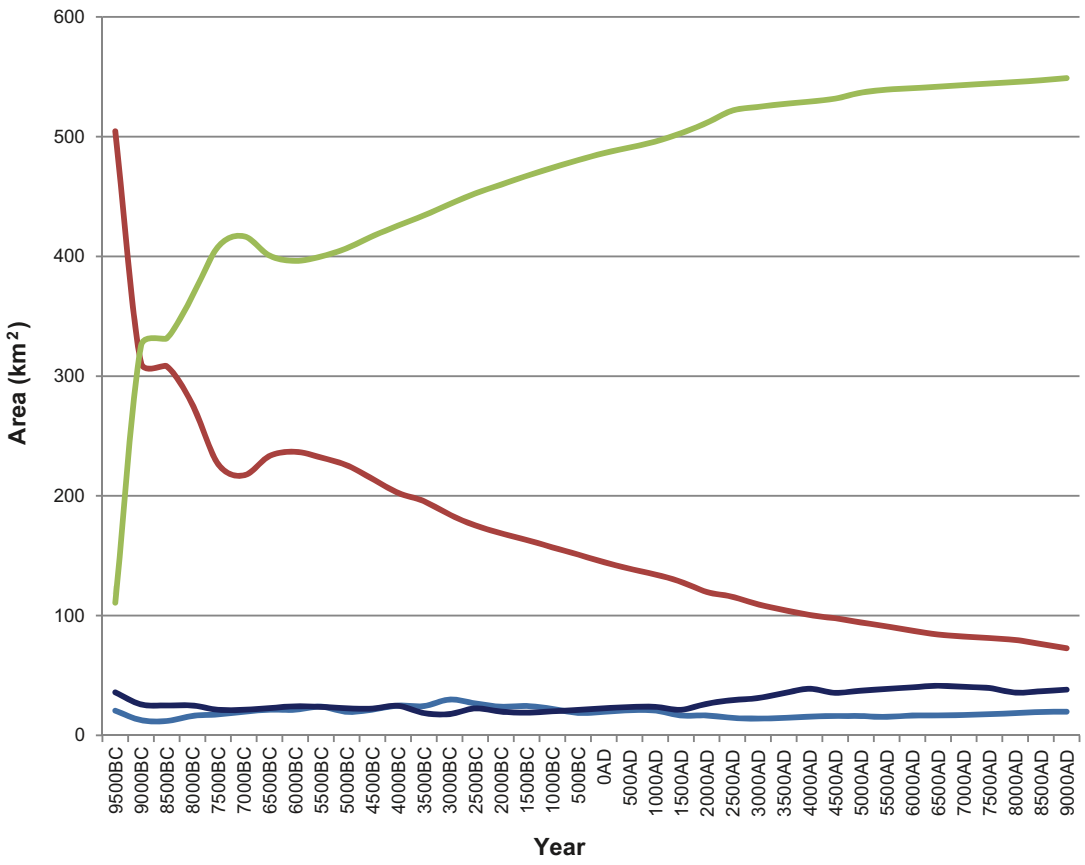

Figure 3-10. *Change in area extensions over time in three bottom types at the Laxemar site.*

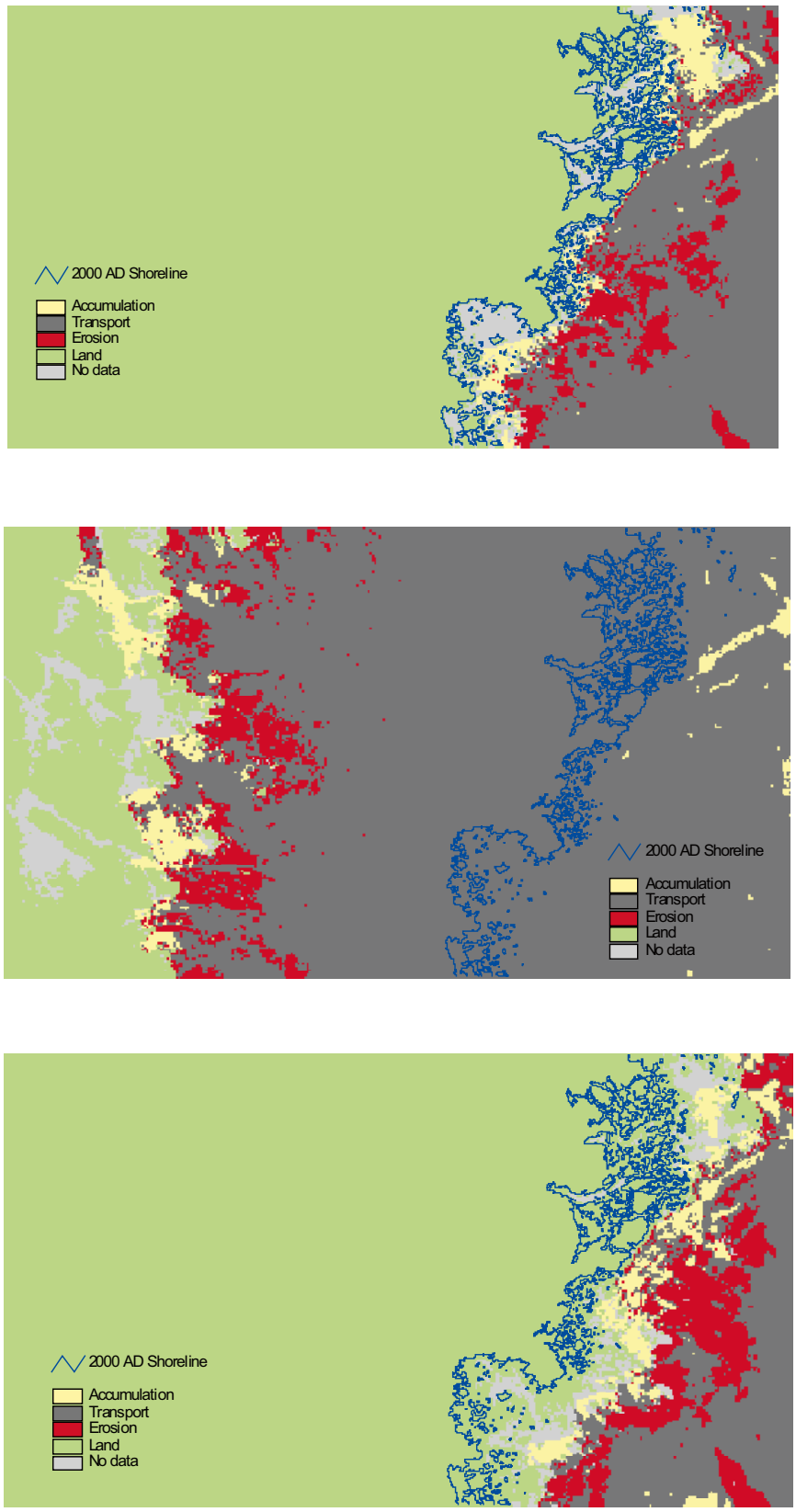

Figure 3-11 Extensions of modelled different bottom types in Laxemar at 2000 AD (top), 9500 BC (middle), and 9500 AD (bottom). *The thin blue line is the shoreline in 2000 AD.*

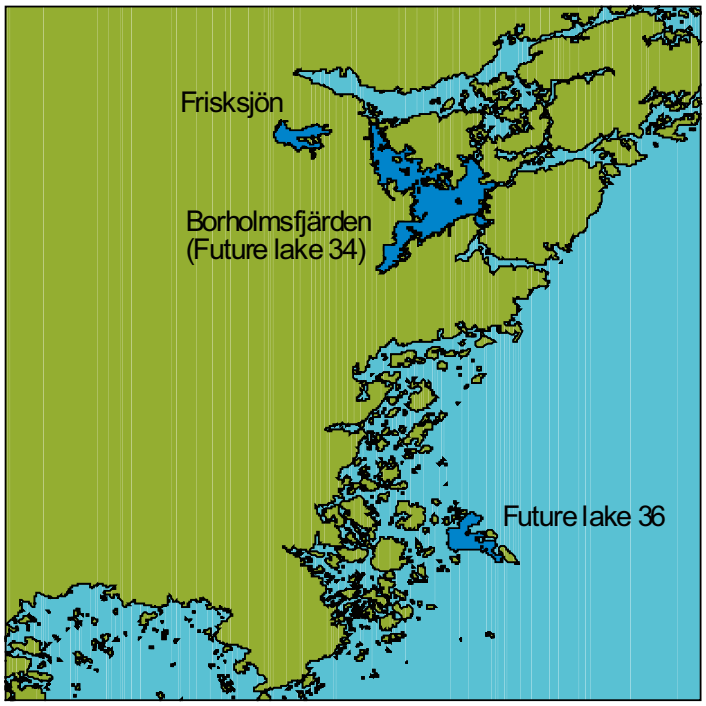

Figure 3-12. *Location of an existing lake (Frisksjön) and two futures lakes, one close to an isolation phase (Borholmsfjärden) and one that will be isolated c. 7400 AD. The two future lakes will have different physical characteristics (e.g. water volumes and maximum water depths).*

Figure 3-13 shows the distribution of different bottom types for three periods; 9500 BC, 2000 AD and 9500 AD. The same pattern is to be found in all three time steps:

(i) Accumulation bottoms are found close to the shore in semi-enclosed bays or on leeside of larger islands (The most powerful waves are from NE, so leeside is on the SW sides of islands). Accumulation bottoms can also be found in the deepest parts of the open sea.

(ii) Erosion bottoms occur on shallow bottoms exposed to waves from N – E.

(iii) Transport bottoms are found in a wide belt in intermediate water depths between the erosion bottoms and the deep-sea accumulation bottoms.

This pattern moves from east to west over time so most of the places within the domain have had a sedimentation history of transitions: accumulation – transport – erosion – accumulation – land.

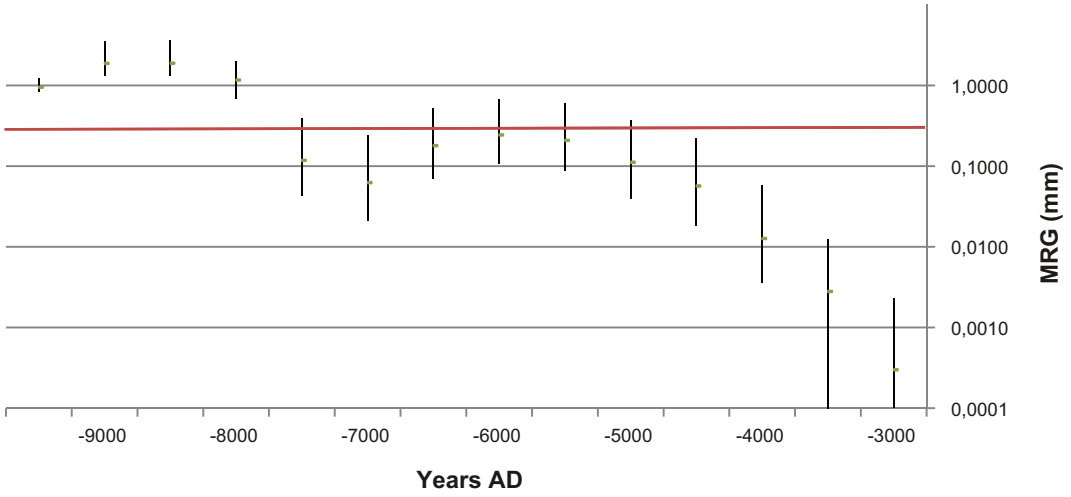

Figure 3-13. *A MRG – time diagram (min – average – max) for the Lake Frisksjön (see Figure 3-12). MRG = Maximum Resuspendable Grain size.*

Figure 3-13 shows the change over time in sedimentation climate for Lake Frisksjön. The lake had an erosion climate until approximately 7750 BC. After 7750 BC, the lake had an accumulation climate in part of or in the whole lake. Note that the lake has been affected by focusing (maximum value above the red line and minimum value below) during a long period, which could explain the extraordinary thick strata of fine-grade sediments observed in part of the lake (> 7 m) /Nilsson 2004/.

The overall patterns in MRG change over time are the same for Frisksjön and Borholmsfjärden, patterns that are expected since they are situated close to each other and approximately at the same elevation. Despite this, the differences in heights of the overall patterns relative the threshold MRG-value (0.27 mm) generate different sediment features. While the Lake Frisksjön show a long period with focusing, the Borholmsfjärden was dominated by erosion during the same period, which possibly results in thinner strata of fine-grained sediment (~5 m) /Risberg 2002/.

Future Lake 36 will be an intermediate sized lake (compared to other future lakes in the domain), but rather deep with average depth of 3.4 meters and a maximum depth of 10.5 meters. The overall MRG-time pattern is similar to Frisksjön and Borholmsfjärden, but the deeper lake basin will have a larger range in MRG-values resulting in longer periods with focusing. After 10,000 years of accumulation, the basin is now switching to an erosion cycle. Therefore, the deepest part of the basin fine-grained sediment can probably be found. Unfortunately, this cannot be confirmed since there are no marine geological survey maps of the area.

Obviously, the two sites differ greatly in the way the sedimentation climate has changed over time (compare e.g. Figures 3-1 and 3-10). One way to show this in a single diagram is to calculate the change in focusing over time for the two sites. Normally, the focusing concept is used for sediments in lakes and means fine-grained particles are concentrated to the deeper parts of the lake by resuspension of sediments in shallower zones and transport to and settling in deeper zones /Likens and Davis 1975/. This concept can also be applied to the sea. Although the export of resuspended particles out of a lake is a simple measurement, quantifying the export/import of particles from/to a sea domain is much more complicated. The export/import of particles from/to the Forsmark and Laxemar model are unknown; however, by expressing the focusing as the sum of areas of erosion and transport bottoms divided by the total area of sea bottoms, it is possible to show the change in strength over time of the focusing processes.

The focusing diagrams for the two sites are totally different. The focusing factor for Forsmark increases from zero up to 100% and back to zero along the period, whereas the factor for Laxemar decreases slowly from 97% to 85%. A low focusing value means that the contamination of radionuclides is spread over a larger area compared to a period with high focusing where the contaminated particles could be concentrated to a small area with accumulation environment.

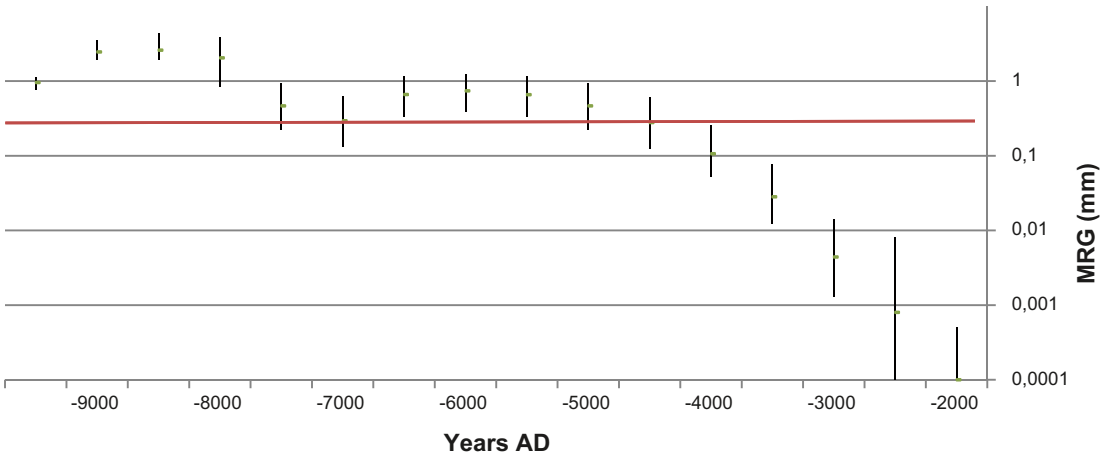

Figure 3-14. *A MRG – time diagram (min – average – max) for the Lake Borholmsfjärden (see Figure 3-12). MRG = Maximum Resuspendable Grain size.*

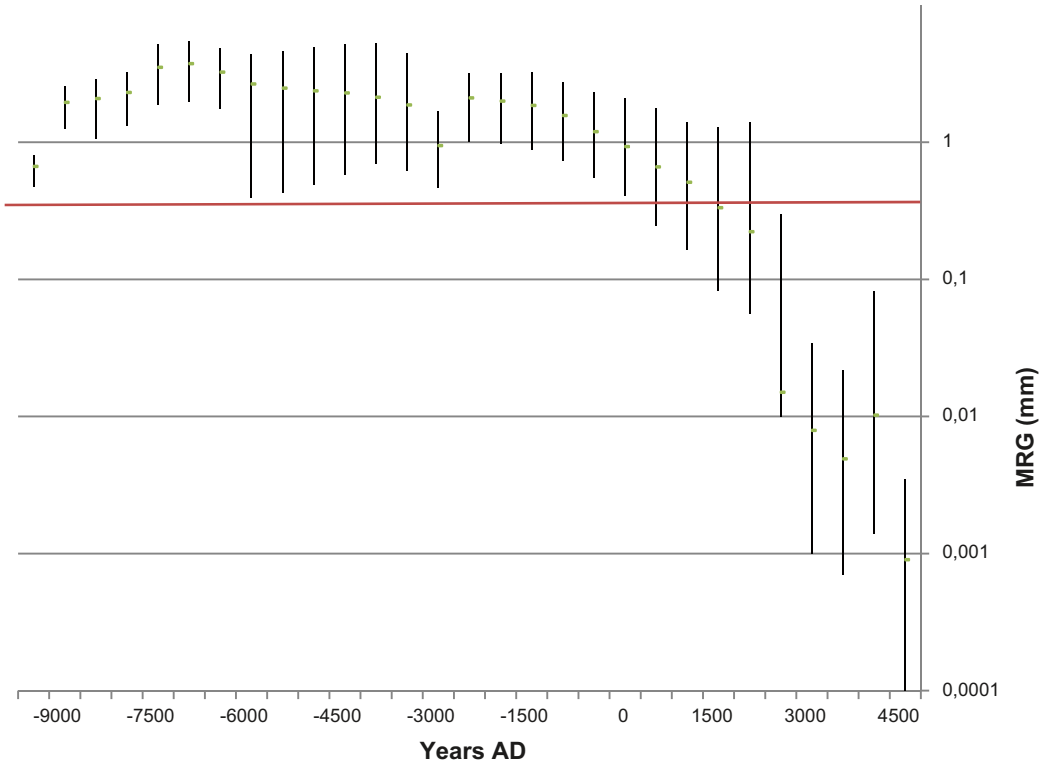

Figure 3-15. *A MRG – time diagram (min – average – max) for the Future lake 36 (see Figure 3-12). MRG = Maximum Resuspendable Grain size.*

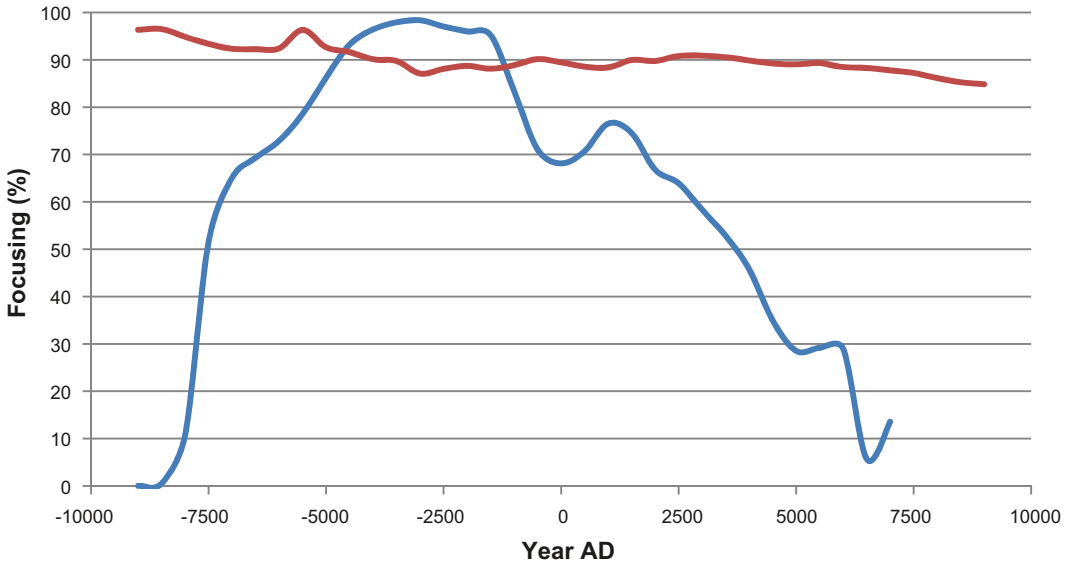

Figure 3-16. *Change in degree of focusing over time for Forsmark (blue line) and Laxemar (red line).*

4 Discussion

The choice of delimiting wind speeds for simulations of bottom types (10 and 25 m s^{-1}) is conservative. This means that the area extensions of transport bottoms are overestimated and areas of erosion and accumulation bottoms are underestimated. To get an apprehension of how sensitive these choices are for the simulation results, all wind speeds between 5 and 30 m s^{-1} were simulated for the Forsmark site for the time step 2000 AD (see Figure 4-1). The figure shows the areas of erosion bottoms for different wind speeds.

The area of erosion bottoms increases fast from a wind speed of about 8 m s^{-1} up to about 12 m s^{-1} and then only increases slowly for higher wind speeds. This implies that the delimiting wind speeds for distinguishing between erosion and transport bottoms are highly sensitive but not the delimiting wind speed for separate accumulation bottoms from transport bottoms. As a consequence, the areas of erosion bottoms can be highly underestimated. This is of minor importance for most applications since the important question is whether the contaminated particle is settled forever or for a limited time, but if it is important to know whether the particle is settled for one month, one year, or 500 years, the choice of the lower delimiting wind speed is essential.

Some sediment characteristics found in marine geological surveys sediment characteristics of a deep sediment core sampled in the Gräsörännan at the Forsmark site /Risberg 2005/ cannot be explained with results from the simulations. C^{14} dating shows at least two periods with extensive erosion during the Holocene whereas the resuspension model shows an unbroken period with accumulations. This discrepancy is probably caused by unidirectional baroclinic currents. As mentioned earlier, the model is not capable to detect resuspension due to unidirectional currents nor can it use the combined water movement of waves and currents. If the wave generated water movement is the dominating process for resuspension /Komar and Miller 1975/, it is likely at some topographical places (capes, narrow channels, etc) that the unidirectional currents can interact with waves in the resuspension process.

The limitation of the sediment dynamic model is due to the lack of wind driven 3D current models with a resolution in water depth that gives a correct description of the currents close to the sediment surface, which can be combined with the STWAVE model. If this combined model could be set up in the future, it should be possible to detect whether resuspension is the result of waves or currents or a combination of the two. The next step should be analyses of the effect of future change in climate of the sediment dynamics in coastal zones.

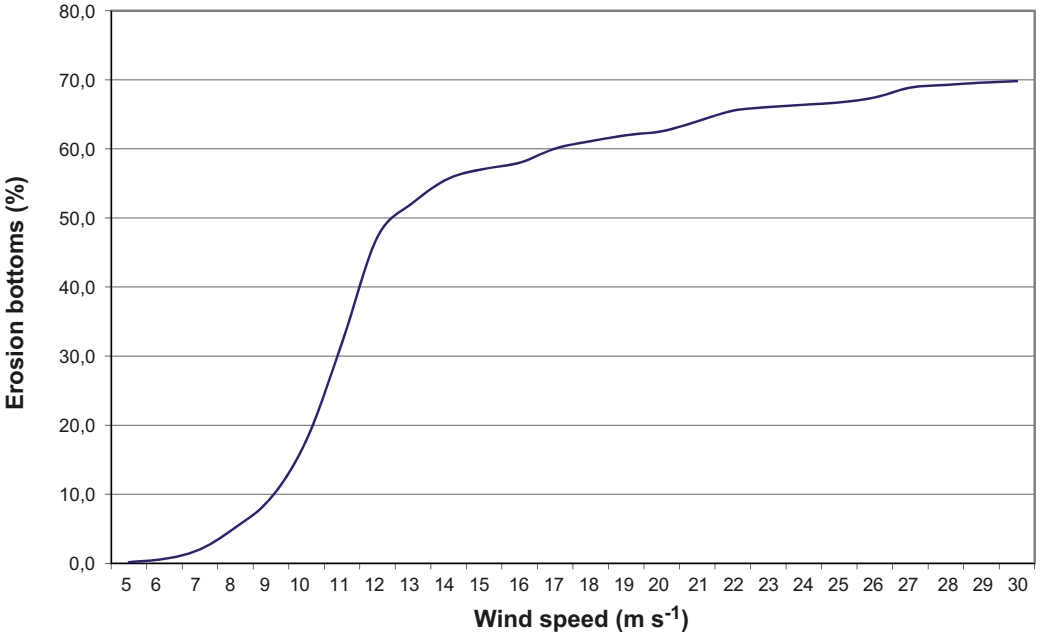

Figure 4-1. *The relationship between wind speed and share of bottoms classified as erosion bottoms.*

Another sediment feature that differs from the model results are found on the northwest side of Gräsö at the Forsmark site. The area is mapped as glacial clay, bedrock, or till but modelled as accumulation bottom. The till in the area is characterized by many large boulders, many larger than three meters in diameter. The STWAVE depth grid cannot correctly represent that type of bottom due to the grid size of 100 meters. On these types of bottoms (very common in Forsmark), the water velocity in between the boulders is much higher than modelled, so the extension of the modelled accumulation bottoms will be overestimated. Using a STWAVE depth grid with higher resolution (50 or 25 meters) will not solve this problem, but based on a marine geological map where the boulder content is included, these bottoms can be reclassified as transport bottoms or marked as "Uncertain bottom type".

A third type of discrepancies between geological maps and model results are found in shallow open sea areas in Laxemar. The geological survey detects bedrock outcrops although the model predicts clay or silt (accumulation bottom). Common for many of these sites are a late switch from transport to accumulation bottoms. It seems that fine-grained particles have less ability to settle directly on a bedrock surface compared to till or glacial clay surfaces. The sonar record from the geological survey shows that bedrock overlaid by postglacial clay exists, but this rarely happens /Elhammer and Sandqvist 2005b/. Perhaps different delimiting MRG-values should be used to distinguish between transport bottoms and accumulation bottoms depending on the property of the existing geology.

The figure showing change over time in focusing for the two sites (Figure 3-16) is calculated with an export of fine-grained particles out from the coastal areas set to zero. Of course, this is not correct, but is set to zero because the net export is unknown. It is important that the magnitude of these flows can be quantified, especially at a comparison of the focusing between the two sites. The export is probably much larger at the Laxemar site where few accumulation bottoms "survive" and becomes postglacial clay or silt sediments on land. In my opinion there are two techniques available to solve this problem:

(i) A current model that can be combined with a wave model and together build up a "particle tracker model" could address this concern. Future versions of the SMS program suite will include 3D current models that can be run simultaneously with the STWAVE model and driven with exactly the same weather data. When this 3D-model will be available is uncertain and it is unclear if my resuspension module can be added to the combined model structure. Another option is to use the DHI program MIKE21 that already has a developed coupled model (wave, current, resuspension, and particle tracking).

(ii) A mass balance model for fine-grained particles for the two sites could also address this concern. Here is an outline of the mass balance model could be used:

Net export = Fine-grained particles "missing" in the till + fluvial import to the coastal area – postglacial fine-grained particles in coastal sea sediments.

The fluvial term is probably small compared to the wave wash term so the goal is to calculate the other two terms. The requirements are rather good; the till are sampled and analyzed for grain size at many locations and the sonar surveys in the coastal areas can be used to calculate the mass of post-glacial fine-grained sediments. One major problem will be the delimitation of the model domains.

References

Brydsten L, 1985. Om stränder – Processer, material och former. GERUM Nr. 1.

Brydsten L, 1999. Change in coastal sedimentation conditions due to positive shore displacement in Öregrundsgrepen. SKB TR-99-37. Svensk Kärnbränslehantering AB.

Brydsten L, 2006. A model for landscape development in terms of shoreline displacement, sediment dynamics, lake formation, and lake choke-up processes. SKB TR-06-40. Svensk Kärnbränslehantering AB.

Elhammer A, Sandkvist Å, 2005a. Detailed marine geological survey of the sea bottom outside Forsmark. Forsmark site investigation. SKB P-03-101. Svensk Kärnbränslehantering AB.

Elhammer A, Sandkvist Å, 2005b. Detailed marine geological survey of the sea bottom outside Simpevarp. Oskarshamn site investigation. SKB P-05-35. Svensk Kärnbränslehantering AB.

Engqvist A, Andrejev O, 1999. Water exchange of Öregrundsgrepen. A baroclinic 3D-model study. SKB TR-99-11. Svensk Kärnbränslehantering AB.

Hedenström A, 2004. Investigation of marine and lacustrine sediment in lakes. Stratigraphical and analytical data. Forsmark site investigation. SKB P-04-86. Svensk Kärnbränslehantering AB.

Hedenström A, Risberg J, 2003. Shore displacement in northern Uppland during the last 6500 calender years. SKB TR-03-17. Svensk Kärnbränslehantering AB.

Likens G E, Davis M B, 1975. Post-glacial history of Mirror Lake and its watershed in New Hampshire, USA: An initial report. Int. Ver. Theor. Angew. Limnol. Vcrh. 19: 982-993.

Komar P D, Miller M C, 1973. The threshold of sediment movement under oscillatory water waves. J. Sediment. Petrol., 43:1101-10.

Komar P D, Miller M C, 1975. On the comparision between the threshold of sediment motion under waves and unidirectional currents with a discussion of the practical evaluation of the threshold. J. Sediment. Petrol., 45:363-367.

May J P, 1974. WAVENRG: A computer program to determine the distribution of energy dissipation in shoaling water waves with examples from coastal Florida. In: Sediment transport in the near shore zone. Florida bureau of geology. Tallahasse, 22–79.

McKee Smith J, Sherlock A R, Resio D T, 2001. STWAVE: Steady-State Spectral Wave Model. User's Manual for STWAVE, Version 3.0. Coastal and Hydraulics Laboratory U.S. Army Engineer Research and Development Center.

Militello A, Reed C W, Zundel A, 2004. Two-Dimensional Depth-Averaged Circulation Model M2D: Version 2.0, Report 1, Technical Documentation and User's Guide. Coastal and Hydraulics Laboratory U.S. Army Engineer Research and Development Center.

Nilsson G, 2004. Investigation of sediments, peat lands and wetlands. Stratigraphical and analytical data. Oskarshamn site investigation. SKB P-04-273. Svensk Kärnbränslehantering AB.

Påsse T, 2001. An empirical model of glacio-isostatic movements and shore-level displacement in Fennoscandia. SKB R-01-41. Svensk Kärnbränslehantering AB.

Risberg J, 2002. Holocene sediment accumulation in the Äspö area. A study of a sediment core. SKB R-02-47. Svensk Kärnbränslehantering AB.

Risberg J, 2005. Bio- and lithostratigraphy in offshore sediment core PFM004396. Salinity variations in the Bothnian Sea offshore Forsmark. Forsmark site investigation. SKB P-05-139. Svensk Kärnbränslehantering AB.

Seifert T, Tauber F, Kayser B, 2001. A high resolution spherical grid topography of the Baltic Sea – revised edition, Proceedings of the Baltic Sea Science Congress, Stockholm 25-29.

Silvester R, 1974. Coastal Engineering, 1. Generation, propagation and influence of waves. Elsivire, Amsterdam.

Strömgren M, Brydsten L, 2008a. Digital elevation models of Forsmark. Site descriptive modelling. SDM-Site Forsmark. SKB R-08-62. Svensk Kärnbränslehantering AB.

Strömgren M, Brydsten L, 2008b. Digital elevation models of Laxemar/Simpevarp. Site descriptive modelling. SDM-Site Laxemar/Simpevarp. Svensk Kärnbränslehantering AB.

Söderbäck B (ed), 2008. Geological evolution, palaeoclimate and historical development of the Forsmark and Laxemar-Simpevarp areas. Site descriptive modelling. SDM-Site. SKB R-08-19.

Appendix

Average number of yearly events at Laxemar, Bothnian Bay, Bothnian Sea, N. Baltic Proper and NW Baltic Proper with wind speeds (m s–1) and wind durations (h) exceeding certain values. Only wind directions from 340–70 º are analyzed. Data for Forsmark are displayed in Figure 2-2.

Laxemar

	Wind speed	> 10	> 11	> 12	> 13	> 14	> 15	> 16	> 17	> 18	> 19	> 20	> 21	> 22	> 23	> 24	> 25	> 26
Duration	**> 6**	349	260	195	140	100	72	48	32	21	13	9	6	4	2	1	1	< 1
	> 9	278	204	149	104	71	50	31	20	12	8	5	3	2	1	1	< 1	< 1
	> 12	223	160	114	76	50	34	20	13	8	4	3	2	1	1	< 1	< 1	
	> 15	178	124	85	55	34	23	14	8	4	2	1	1	< 1	< 1	< 1	< 1	
	> 18	143	96	64	39	23	16	9	5	3	1	1	< 1	< 1	< 1			
	> 21	116	75	49	28	16	11	6	3	1	< 1	< 1	< 1					
	> 24	93	58	37	20	11	7	4	2	1	< 1	< 1	< 1					
	> 27	76	45	27	14	7	5	2	1	< 1	< 1	< 1						
	> 30	62	35	20	10	5	3	2	< 1	< 1								
	> 33	50	27	14	7	3	2	1	< 1									
	> 36	40	20	10	5	2	1	1										
	> 39	32	15	8	4	1	1	< 1										
	> 42	26	12	6	3	1	1	< 1										
	> 45	21	9	5	2	1	< 1	< 1										
	> 48	16	7	3	1	< 1	< 1	< 1										
	> 51	13	5	3	1	< 1	< 1	< 1										
	> 54	9	4	2	1	< 1	< 1	< 1										
	> 57	7	3	1	1	< 1	< 1											
	> 60	5	3	1	< 1													
	> 63	4	2	1	< 1													
	> 66	4	2	1	< 1													

Bothnian Bay

	Wind speed	> 10	> 11	> 12	> 13	> 14	> 15	> 16	> 17	> 18	> 19	> 20	> 21	> 22	> 23	> 24	> 25	> 26	> 27	> 28
Duration	**> 6**	386	296	224	169	126	92	65	43	30	20	12	8	5	2	1	1	1	< 1	< 1
	> 9	312	235	174	128	93	67	46	29	19	12	7	4	3	1	1	< 1	< 1	< 1	
	> 12	251	185	134	96	68	49	32	20	12	7	4	2	1	< 1	< 1	< 1	< 1		
	> 15	204	147	104	73	51	36	23	14	8	5	2	1	1	< 1					
	> 18	166	118	81	56	38	27	16	9	5	3	1	< 1	< 1						
	> 21	136	94	63	43	28	19	11	6	3	1	1	< 1							
	> 24	112	75	49	33	21	14	8	4	2	1	< 1	< 1							
	> 27	92	60	38	25	15	10	6	3	1	< 1	< 1	< 1							
	> 30	76	48	30	18	11	7	4	2	1	< 1	< 1								
	> 33	63	38	23	13	7	5	3	1	1	< 1	< 1								
	> 36	52	30	17	10	5	3	2	1	< 1	< 1									
	> 39	44	24	14	7	4	2	1	< 1	< 1										
	> 42	38	19	11	5	3	2	1	< 1	< 1										
	> 45	32	16	9	4	2	1	1	< 1	< 1										
	> 48	28	13	7	3	1	1	1	< 1	< 1										
	> 51	24	10	6	2	1	1	< 1	< 1											
	> 54	21	8	5	2	1	< 1	< 1												
	> 57	18	7	4	1	1	< 1	< 1												
	> 60	15	5	3	1	1	< 1													
	> 63	13	4	2	1	< 1														
	> 66	11	3	2	< 1	< 1														

Bothnian Sea

	Wind speed	> 10	> 11	> 12	> 13	> 14	> 15	> 16	> 17	> 18	> 19	> 20	> 21	> 22	> 23	> 24	> 25
Duration	**> 6**	261	189	134	90	60	39	24	15	9	5	3	1	1	< 1	< 1	< 1
	> 9	205	145	99	65	40	25	15	9	5	3	1	1	< 1	< 1		
	> 12	162	111	73	46	27	16	10	5	3	1	1	< 1				
	> 15	126	84	54	32	18	11	6	3	1	1	< 1					
	> 18	98	65	40	22	12	7	4	2	1	< 1						
	> 21	76	50	29	15	8	4	2	1	< 1							
	> 24	60	39	21	11	6	3	1	1	< 1							
	> 27	47	30	15	8	4	2	1	< 1								
	> 30	36	23	11	5	3	1	< 1	< 1								
	> 33	29	17	8	4	2	1	< 1									
	> 36	23	14	6	3	2	< 1	< 1									
	> 39	19	12	5	2	1	< 1										
	> 42	17	10	4	2	1	< 1										
	> 45	14	8	3	1	< 1											
	> 48	12	7	2	1	< 1											
	> 51	11	5	2	< 1												
	> 54	9	4	1	< 1												
	> 57	8	3	1													
	> 60	7	2	< 1													
	> 63	6	2														
	> 66	5	1														

NW Baltic Proper

	Wind speed	> 10	> 11	> 12	> 13	> 14	> 15	> 16	> 17	> 18	> 19	> 20	> 21	> 22	> 23	> 24	> 25	> 26	> 27	> 28	> 29	> 30	> 31
Duration	**> 6**	443	345	265	196	141	100	73	52	35	23	14	10	7	4	3	2	<1	< 1	< 1	< 1	< 1	< 1
	> 9	365	280	211	152	106	73	53	35	21	14	8	5	3	2	1	1	< 1	< 1	< 1			
	> 12	300	227	167	117	79	53	36	22	12	8	4	3	2	1	1	< 1	< 1					
	> 15	249	184	132	89	57	37	24	13	7	4	2	2	1	1	< 1	< 1						
	> 18	207	149	104	66	41	27	16	8	4	2	1	1	1	< 1	< 1	< 1						
	> 21	171	121	81	49	30	19	11	5	2	1	1	1	< 1	< 1								
	> 24	142	97	63	37	22	14	7	3	1	1	1	< 1	< 1									
	> 27	117	78	49	28	16	10	5	2	1	1	< 1	< 1	< 1									
	> 30	97	63	38	21	11	7	3	1	< 1	< 1	< 1											
	> 33	80	51	29	15	8	5	2	< 1	< 1	< 1												
	> 36	66	41	22	11	6	3	1	< 1														
	> 39	54	32	17	8	4	2	< 1	0														
	> 42	44	26	13	6	3	1																
	> 45	36	21	10	5	2	1																
	> 48	30	16	8	4	1	< 1																
	> 51	24	13	6	3	1	< 1																
	> 54	19	10	5	3	1	< 1																
	> 57	15	8	4	2	< 1	< 1																
	> 60	12	6	3	2	< 1	< 1																
	> 63	10	5	3	1																		

N Baltic Proper

	Wind speed	> 10	> 11	> 12	> 13	> 14	> 15	> 16	> 17	> 18	> 19	> 20	> 21	> 22	> 23	> 24	> 25	> 26	> 27	> 28	> 29	> 30	> 31	> 32	> 33	> 34	> 35	> 37	> 38	> 39
Duration	**> 6**	540	427	331	249	186	138	102	76	55	40	27	19	13	9	6	4	3	2	2	1	1	1	1	< 1	< 1	< 1	< 1	< 1	< 1
	> 9	449	349	263	192	140	101	72	52	35	25	16	10	7	5	3	2	1	1	1	1	< 1	< 1	< 1	< 1	< 1				
	> 12	374	285	210	149	105	73	50	34	22	15	9	6	4	2	1	1	1	< 1	< 1	< 1	< 1	< 1	< 1	< 1	< 1				
	> 15	312	233	166	114	79	53	35	22	14	9	5	3	2	1	1	1	< 1	< 1	< 1	< 1	< 1								
	> 18	262	191	133	88	59	38	24	14	8	5	3	2	1	1	< 1	< 1	< 1	< 1	< 1	< 1	< 1								
	> 21	220	157	107	69	45	28	16	9	5	3	2	1	< 1	< 1	< 1	< 1	< 1	< 1	< 1	< 1									
	> 24	185	129	86	53	34	20	12	6	3	2	1	< 1	< 1	< 1	< 1	< 1	< 1												
	> 27	155	106	68	41	26	15	8	3	2	1	< 1	< 1	< 1	< 1	< 1	< 1													
	> 30	130	87	54	31	19	11	6	2	1	1	< 1	< 1																	
	> 33	109	71	44	24	14	8	4	1	< 1	< 1																			
	> 36	92	58	34	19	11	6	3	1	< 1	< 1																			
	> 39	78	47	27	15	8	5	2	< 1	< 1																				
	> 42	66	39	23	13	6	4	2	< 1																					
	> 45	56	32	19	10	5	3	1	< 1																					
	> 48	47	26	16	9	4	2	1																						
	> 51	40	22	13	8	4	2	1																						
	> 54	33	18	11	7	3	1	1																						
	> 57	28	16	10	6	2	1	1																						
	> 60	24	14	8	5	2	1	< 1																						
	> 63	20	12	7	4	1	1	< 1																						
	> 66	17	10	6	4	1	< 1	< 1																						

ISSN 1404-0344
CM Gruppen AB, Bromma, 2009